

# Stability of Kink Defects in a Deformed $O(3)$ Linear Sigma Model

†A. Alonso Izquierdo, †M.A. González León  
and ‡J. Mateos Guilarte

†DEPARTAMENTO DE MATEMÁTICA APLICADA

‡DEPARTAMENTO DE FÍSICA

Universidad de Salamanca, SPAIN

## Abstract

We identify the kinks of a deformed  $O(3)$  linear Sigma model as the solutions of a set of first-order systems of equations; the above model is a generalization of the MSTB model with a three-component scalar field. Taking into account certain kink energy sum rules we show that the variety of kinks has the structure of a moduli space that can be compactified in a fairly natural way. The generic kinks, however, are unstable and Morse Theory provides the framework for the analysis of kink stability.

# 1 Introduction

In Reference [1] we investigated the solitary waves that arise in a deformed  $O(3)$  linear Sigma model. These non-linear waves appear as kink defects when the system is considered in a  $(1+1)$ -dimensional space-time. The research performed in [1] was based on study of the Hamilton-Jacobi equation of the mechanical analogue system that follows when time-independent field configurations are considered. Interest in this model was explained in our previous work [1], and the physical meaning of the kinks was also discussed. Our aim in the present paper is to gain a better understanding of the nature of such a rich variety of kinks. We shall focus on three important aspects:

I. In order to clarify the origin of the kink-energy sum rules we shall develop a treatment à la Bogomolny [2] rather than applying the Hamilton-Jacobi method as in [1]. The system, which is a generalization of the MSTB model to a three-component scalar field, is the Bosonic sector of a super-symmetric system: the interaction energy is derived from a super-potential (in fact, this property is not exclusive of the three-component case: the  $N$ -component analogue model is also the Bosonic sector of a super-symmetric theory). Thus, the time-independent solutions satisfy a set of systems of first-order ODE that, of course, is equivalent to the ODE system obtained in the framework of the Hamilton-Jacobi paradigm. The bonus of this approach is double: first, the appearance of the kink energies as several Bogomolny bounds clarifies the fact that the energy of a generic kink is equal to the sum of the energies of two or three non-generic kinks in several ways and, second, the Bogomolny formulation allows us to prove the stability of one of the kink solutions: the absolute minimum of the energy in the appropriate topological sector.

II. There is a symmetry group in the system that is generated by the transformations  $\phi_a \rightarrow (-1)^{\delta_{ab}} \phi_b$ ,  $b = 1, 2, 3$ , where  $\phi_a$ ,  $a = 1, 2, 3$ , are the three components of the field. This group,  $G = \mathbb{Z}_2 \times \mathbb{Z}_2 \times \mathbb{Z}_2$ , acts on the variety of kink solutions, which are classified into three types; see [1]:

1. Generic kinks. There are two three-parametric families of topological kink trajectories whose three components are non-null. For obvious reasons, they are usually termed as TK3 kinks. We shall use the term kink orbit, or simply kink, to denote the kink solution without specifying the spatial dependence. From this point of view, TK3 kinks are two two-parametric families of kink orbits and two three-parametric families of kink trajectories or solitary waves.

2. Enveloping kinks. There are four one-parametric families of non-topological kink orbits that also have three non-null components. NTK3 kinks live on one ellipsoid in the  $\mathbb{R}^3$  internal space that encloses all the other kinks.

3. Embedded kinks. All the solitary waves of the  $N = 2$  MSTB model appear embedded twice in the kink manifold of the  $N = 3$  system. Thus, these kinks have at most two non-null components. There are two classes: a) Two-component non-topological and topological kinks. The NTK2 kink orbits form two one-parametric families in the  $\phi_3 = 0$  plane and another two one-parametric families in the  $\phi_2 = 0$  plane. TK2 kinks appear at a limit of these two families that we shall explain later. b) One-component topological kinks. There exists one topological TK1 kink and one anti-kink both of which live on the  $\phi_1$ -axis.

We briefly describe the action of  $G$  on a given kink, starting in the opposite order:

- One-component topological kinks and anti-kinks are fixed points of the action of the elements  $\phi_2 \rightarrow -\phi_2$ ,  $\phi_3 \rightarrow -\phi_3$ . The transformation  $\phi_1 \rightarrow -\phi_1$ , however, sends a TK1

kink to its anti-kink, and vice-versa.

- The NTK2 families are invariant under the action of either  $\phi_3 \rightarrow -\phi_3$  or  $\phi_2 \rightarrow -\phi_2$ .  $\phi_1 \rightarrow -\phi_1$  exchanges the families living in the same plane. Finally,  $\phi_2 \rightarrow -\phi_2$  sends one NTK2 kink of the  $\phi_3 = 0$  plane to another in the same family, all of them invariant under  $\phi_3 \rightarrow -\phi_3$ . We find the same situation with the NTK2 family in the  $\phi_2 = 0$  plane with respect to  $\phi_3 \rightarrow -\phi_3$  and  $\phi_2 \rightarrow -\phi_2$ , respectively.
- The four NTK3 families are interchanged through the action of  $\phi_1 \rightarrow -\phi_1$  and  $\phi_3 \rightarrow -\phi_3$ .  $\phi_2 \rightarrow -\phi_2$ , however, relates two NTK3 kinks in the same family.
- The two TK3 families are related by the  $\phi_1 \rightarrow -\phi_1$  transformation.  $\phi_2 \rightarrow -\phi_2$  and  $\phi_3 \rightarrow -\phi_3$  link two TK3 kinks in the same family.

The moduli space of kinks is the quotient of the variety of kinks by the action of the  $G$  group. Restriction to the sub-variety of generic kinks leads to a good structure for the kink moduli sub-space because there are no fixed points. We shall show (see also [1]) that the kink solutions are obtained using Jacobi elliptic coordinates in the internal  $\mathbb{R}^3$  space. The sub-space of TK3 kink orbits in elliptic coordinates is parametrized by two real integration constants. Thus, the TK3 moduli sub-space is the open  $\mathbb{R}^2$  plane. Because the change from Cartesian to elliptic coordinates is generically a 2<sup>3</sup>-to-1 map, a point in  $\mathcal{M}_{\text{TK3}} = \mathbb{R}^2$  corresponds to eight TK3 kinks, which precisely form an orbit -in the sense of group action- of the  $G$  group.

There are identities between the energy of a generic kink and the sum of one embedded kink and one enveloping kink, or the sum of several embedded kinks, in several ways. The combinations of the embedded and the enveloping kinks are singular in the sense that they are fixed points of some sub-group of  $G$ . Fortunately, one can see that the singular configurations are a limiting case of TK3 kinks that appear in the “boundary” of the TK3 moduli sub-space. This situation calls for a compactification of  $\mathcal{M}_{\text{TK3}}$  and we shall describe how it is possible to include the whole variety of kinks in a compact moduli space.

We thus find analogies with the Mumford-Deligne compactification of the moduli space of Riemann surfaces of genus  $g$ , [4]. Also, the kink moduli space is a similar structure to the moduli space of instantons in pure gauge theory, [5], or of BPS monopoles in Yang-Mills-Higgs systems, [6]: the discrete group  $G$  replaces the infinite dimensional diffeomorphism group in the case of surfaces, or the gauge group in the other cases. The orbit of every point in the kink moduli space is a discrete set; the main difference with respect to the gauge theoretical analogues, however, is that in the system under consideration there are no solutions with several kinks and therefore the moduli space only encompasses the sectors of topological charges  $Q_T = \pm 1$ .

III. There is another difference with the gauge theory solitons mentioned above: both the instantons and the BPS magnetic monopoles are absolute minima of either the Euclidean action or the energy, and are thus completely stable. The TK3 kinks, however, are not absolute minima of the energy; in fact, we will show that they are unstable. Study of the stability of the different types of kinks is the main concern of this paper. We shall analyze the stability problem, which is crucial in order to envisage the nature of the quantum states built around the classical kinks in three stages:

- The eight super-potentials that determine eight systems of first-order equations cannot be differentiated at two “focal” lines: an ellipse in the  $\phi_3 = 0$  plane and a hyperbola in the orthogonal  $\phi_2 = 0$  plane. Kink solutions crossing by any of these curves fail to be absolute minima of the energy in their topological sectors: these solutions are obtained by gluing the solutions of at least two different systems of first-order equations. We shall also show that there are Jacobi fields along these kink orbits with zeroes in the vacuum points and the intersection points with the focal lines. According to one Jacobi theorem, see [11], these kinks are not local minima of the energy and are therefore unstable.
- The direct approach to studying kink stability requires an analysis of the spectrum of the second variation, or Hessian functional. The explicit expression of the Hessian functional is only available for the non-generic topological kinks. In the Schrodinger operator that defines the Hessian quadratic form, the potential well depends on the kink solution; the kink solutions, however, cannot be written in terms of elementary transcendental functions except in the non-generic cases mentioned above. In fact, besides the Jacobi fields, the spectral problem can only be fully solved for the TK1 kink, and, partially, for the TK2 $\sigma_3$  kink. Nevertheless, the information obtained this way fits in with the kink-energy sum rules and with the fact that these non-generic kinks live at the boundary of the TK3 kink moduli space perfectly well.
- Finally, we shall construct the Morse theory for the configuration space, choosing energy as the Morse functional. Knowledge of the Jacobi fields allows an immediate application of the Morse index theorem, as in Reference [8], to identify the Morse index - the dimension of the negative eigen-space of the Hessian - of a kink trajectory with the number of crossing points through the focal ellipse and hyperbola: this count measures the degree of kink instability. Moreover, we can easily proceed and read the homology of the configuration space of the system from the critical point structure of the Hessian, following the pattern developed in [9] for the MSTB model. This procedure affords a direct connection between the existence and fate of topological defects and the topology of the configuration space, which, in turn, reveals many features of the quantum states built from these classical extended objects.

The paper is organized in three Sections. There are three sub-sections in Section §2. §2.1 introduces the model and proposes that the solitary waves satisfy a set of systems of first-order ordinary differential equations. §2.2 solves the system by passing to Jacobi elliptic coordinates. §2.3 discusses the existence of the (several) super-potentials that allow the reduction to the first-order ODE system, describes the kink solutions, and establishes the stability of the absolute minimum of the energy functional. Section §3 is divided into three sub-sections. §3.1 states the kink-energy sum rules. In §3.2 the singular kinks are considered as the limit of generic kinks when some of the integration constants that characterize the variety of solutions tend to infinity. In §3.3 we briefly discuss the results of the two previous sub Sections by showing the compact kink moduli space. The theme of Section §4 is the stability of kinks. In §4.1 we give explicit expressions for the Jacobi fields along the TK3 and NTK trajectories. The zeroes of these fields occur when the kink trajectories cross two focal lines, one an ellipse and the other one an hyperbola. Sub-section §4.2 is devoted to solving the spectral problem for the second-order fluctuation operator around the non-generic topological kinks. In §4.3,

the topological implications of stability are unveiled through the elaboration of a Morse theory of kinks. Finally, some reflections on kink quantization are offered in Section §5.

## 2 Bogomolny equations

Besides the second-order evolution equations, many soliton-like solutions satisfy first-order PD or OD equations in relativistic field theories with relevance in fundamental physics and Cosmology. This interesting discovery is due to a generalization by Bogomolny, [2], of the self-duality equations of Euclidean gauge theory, [5], to other space-time dimensions and other systems. Bogomolny's idea has deep topological roots and leads to very rich spaces of (BPS) states in quantum field theory with extended super-symmetry, see [10]. The purpose of this Section is to show how the kinks discovered in Reference [1] in a deformed  $O(3)$  linear Sigma model also enter this framework.

### 2.1 The model: kink defects and first-order equations

We start by briefly describing the model and characterizing the solitary waves as solutions of a system of first-order ODE. Defining non-dimensional space-time coordinates, fields and physical parameters as in [1], the dynamics of the model is determined by the action functional

$$S = \frac{m^2}{\lambda^2} \int d^2x \left\{ \frac{1}{2} \partial_\mu \vec{\phi} \cdot \partial^\mu \vec{\phi} - \frac{1}{2} (\vec{\phi} \cdot \vec{\phi} - 1)^2 - \sum_{a=1}^3 \frac{1}{2} \sigma_a^2 \phi_a^2 \right\} \quad (1)$$

We also use all the conventions in [1] and focus on the maximally asymmetric case,  $\sigma_1^2 = 0 < \sigma_2^2 < \sigma_3^2 < 1$ , in the range of the manifold parameters  $\sigma_2^2$  and  $\sigma_3^2$ , where the kink manifold is richest.

The mechanical system associated with the search for the solitary wave solutions of the model is completely integrable in the sense of Liouville and all the kink solutions can be found analytically. Here we shall not pursue this line of research; it has been fully developed in [1]. Instead, we assume that there exists a super-potential for the system; i.e., a function  $W(\vec{\phi}) : \mathbb{R}^3 \rightarrow \mathbb{R}$  in the internal space such that:

$$\sum_{a=1}^3 \frac{\partial W}{\partial \phi_a} \frac{\partial W}{\partial \phi_a} = (\vec{\phi} \cdot \vec{\phi} - 1)^2 + \sum_{a=1}^3 \sigma_a^2 \phi_a^2 \quad (2)$$

If this is the case, it is possible to write the energy for static configurations ( $\phi_a = \phi_a(x)$ ) à la Bogomolny, see [2]:

$$\begin{aligned} E[\vec{\phi}] &= \frac{m^3}{\lambda^2 \sqrt{2}} \int dx \left\{ \frac{1}{2} \frac{d\vec{\phi}}{dx} \cdot \frac{d\vec{\phi}}{dx} + \frac{1}{2} (\vec{\phi} \cdot \vec{\phi} - 1)^2 + \frac{1}{2} \sum_{a=1}^3 \sigma_a^2 \phi_a^2 \right\} = \\ &= \frac{m^3}{2\lambda^2 \sqrt{2}} \left[ \int dx \sum_{a=1}^3 \left( \frac{d\phi_a}{dx} - \frac{\partial W}{\partial \phi_a} \right) \left( \frac{d\phi_a}{dx} - \frac{\partial W}{\partial \phi_a} \right) + 2 \int \sum_{a=1}^3 d\phi_a \frac{\partial W}{\partial \phi_a} \right] \quad (3) \end{aligned}$$

Configurations that satisfy the system of first-order equations:

$$\frac{d\phi_a}{dx} = \frac{\partial W}{\partial \phi_a}, \quad (4)$$

do not contribute to the first term in  $E[\vec{\phi}]$  and are also solutions of the second-order equations of the model. The solutions of (4) are kinks of the system if they also comply with the finite energy conditions:

$$\lim_{x \rightarrow \pm\infty} \frac{d\phi_a}{dx} = 0, \quad \lim_{x \rightarrow \pm\infty} \phi_a(x) = v_a, \quad \forall a = 1, 2, 3. \quad (5)$$

where  $\vec{v} \equiv (v_1, v_2, v_3)$  is a vector that belongs to the vacuum manifold  $\mathcal{V}$ .  $\mathcal{V}$  is formed by two vectors  $\vec{v}^\pm \equiv (\pm 1, 0, 0)$  and the existence of two points in  $\mathcal{V}$  classifies the kink solutions into topological and non-topological, see [1] for details.

Every kink orbit traces out a path in the internal  $\mathbb{R}^3$  space. There are two possibilities:

- The super-potential  $W(\vec{\phi})$  is differentiable along the kink path. Thus, the second term in (3) is the integral of an exact differential and Stoke's theorem tells us that it depends on the difference of the values of  $W$  at the path endpoints. The energy is a topological bound and the kinks of this type are absolute minima of  $E[\vec{\phi}]$  and stable against small fluctuations.
- There is a discrete set of points along the kink path where  $W(\vec{\phi})$  is not differentiable. The second term in (3) is only differentiable piece-wise and  $E[\vec{\phi}]$  also depends on the values of  $W(\vec{\phi})$  at those points of non-differentiability; for this type of kinks,  $E[\vec{\phi}]$  is not a topological bound. We cannot say strictly that these kinks are solutions of (4) because the points of non-differentiability of  $W(\vec{\phi})$  are turning points of the the kink orbit. Moreover, in sub-Section §2.3 we shall show that there are eight possible choices of  $W$ . If  $\vec{\phi}(x_0)$  is a point where  $W$  is non-differentiable, a kink is a solution of (4) for  $x \in (x_0 - \epsilon, x_0)$ , with a given choice of  $W$ ; the same kink solves (4) with another choice of  $W$  for  $x \in (x_0, x_0 + \epsilon)$ . These kinks are solutions of the second-order equations but are not absolute minima of  $E[\vec{\phi}]$ . We shall see that not only the non-topological kinks belong to this class, but also many others that live in the topological sectors.

## 2.2 Jacobi elliptic coordinates

We now introduce Jacobi elliptic coordinates in the internal  $\mathbb{R}^3$  space, see [1]. Defining  $\bar{\sigma}_a^2 = 1 - \sigma_a^2$ , we shall denote by  $\mathbf{P}_3(\infty)$  the interior of the infinite parallelepiped  $\bar{\mathbf{P}}_3(\infty) = \partial\bar{\mathbf{P}}_3(\infty) \sqcup \mathbf{P}_3(\infty)$ :

$$-\infty < \lambda_1 \leq \bar{\sigma}_3^2 \leq \lambda_2 \leq \bar{\sigma}_2^2 \leq \lambda_3 \leq 1, \quad (6)$$

Thus the map  $\rho : \vec{\phi} \rightarrow \vec{\lambda}$ , from  $\mathbb{R}^3$  to  $\mathbf{P}_3(\infty)$ , given by the change of coordinates:

$$\begin{aligned} \phi_1^2 &= \frac{(1 - \lambda_1)(1 - \lambda_2)(1 - \lambda_3)}{\sigma_2^2 \sigma_3^2}, & \phi_2^2 &= \frac{(\bar{\sigma}_2^2 - \lambda_1)(\bar{\sigma}_2^2 - \lambda_2)(\bar{\sigma}_2^2 - \lambda_3)}{-\sigma_2^2(\sigma_3^2 - \sigma_2^2)} \\ \phi_3^2 &= \frac{(\bar{\sigma}_3^2 - \lambda_1)(\bar{\sigma}_3^2 - \lambda_2)(\bar{\sigma}_3^2 - \lambda_3)}{\sigma_3^2(\sigma_3^2 - \sigma_2^2)} \end{aligned} \quad (7)$$

sends eight points of  $\mathbb{R}^3$  to one point in  $\mathbf{P}_3(\infty)$  and induces a Riemannian metric in  $\mathbf{P}_3(\infty)$ :  
 $g_{aa}(\vec{\lambda}) = \frac{-f_a(\vec{\lambda})}{4A(\lambda_a)}$ ,  $a = 1, 2, 3$ ,  $g_{ab} = 0, \forall a \neq b$ , where:  $A(\lambda_a) = (\lambda_a - 1)(\lambda_a - \bar{\sigma}_2^2)(\lambda_a - \bar{\sigma}_3^2)$ ,  
and  $f_a(\vec{\lambda}) = \prod_{\substack{b=1 \\ a \neq b}}^3 (\lambda_a - \lambda_b)$ .

The potential energy,  $V(\vec{\phi}) = \frac{1}{2} (\vec{\phi} \cdot \vec{\phi} - 1)^2 + \frac{1}{2} \sigma_2^2 \phi_2^2 + \frac{1}{2} \sigma_3^2 \phi_3^2$ , in elliptic coordinates reads:

$$V(\vec{\lambda}) = \frac{1}{2} \left( \frac{\lambda_1^2(\lambda_1 - \bar{\sigma}_2^2)(\lambda_1 - \bar{\sigma}_3^2)}{(\lambda_1 - \lambda_2)(\lambda_1 - \lambda_3)} + \frac{\lambda_2^2(\lambda_2 - \bar{\sigma}_2^2)(\lambda_2 - \bar{\sigma}_3^2)}{(\lambda_2 - \lambda_1)(\lambda_2 - \lambda_3)} + \frac{\lambda_3^2(\lambda_3 - \bar{\sigma}_2^2)(\lambda_3 - \bar{\sigma}_3^2)}{(\lambda_3 - \lambda_1)(\lambda_3 - \lambda_2)} \right) \quad (8)$$

The crucial question is the following: is there a function  $W(\vec{\lambda})$  such that the potential  $V$  can be written in the form

$$2V(\vec{\lambda}) = g_{11}^{-1} \frac{\partial W}{\partial \lambda_1} \frac{\partial W}{\partial \lambda_1} + g_{22}^{-1} \frac{\partial W}{\partial \lambda_2} \frac{\partial W}{\partial \lambda_2} + g_{33}^{-1} \frac{\partial W}{\partial \lambda_3} \frac{\partial W}{\partial \lambda_3} ? \quad (9)$$

The answer is affirmative if the super-potential  $W(\vec{\lambda})$  is a solution of the PDE:

$$\sum_{a=1}^3 \frac{-4(\lambda_a - 1)(\lambda_a - \bar{\sigma}_2^2)(\lambda_a - \bar{\sigma}_3^2)}{f_a(\vec{\lambda})} \left( \frac{\partial W}{\partial \lambda_a} \right)^2 = \sum_{a=1}^3 \frac{\lambda_a^2(\lambda_a - \bar{\sigma}_2^2)(\lambda_a - \bar{\sigma}_3^2)}{f_a(\vec{\lambda})} \quad (10)$$

Note that (10) is no more than the Hamilton-Jacobi equation, formula (20) in [1], for the Hamilton characteristic function  $W(\vec{\lambda})$ , with no explicit dependence on  $x$ .

Searching for solutions of the form  $W(\vec{\lambda}) = W_1(\lambda_1) + W_2(\lambda_2) + W_3(\lambda_3)$ , (10) becomes three separate ODE:

$$\left( \frac{dW_a}{d\lambda_a} \right)^2 = \frac{\lambda_a^2}{4(1 - \lambda_a)}, \quad \forall a = 1, 2, 3 \quad (11)$$

the ordinary differential equations into which the HJ equation degenerates when all the separation constants are at zero, see formula (29) for  $N = 3$  in [1].

The integration of (11) is elementary:

$$W_a^{(\alpha_a)} = (-1)^{\alpha_a} \int \frac{\lambda_a d\lambda_a}{2\sqrt{1 - \lambda_a}} = -(-1)^{\alpha_a} \frac{1}{3} (\lambda_a + 2) \sqrt{1 - \lambda_a}, \quad \alpha_a = 0, 1,$$

if we set the integration constant to be zero. There is also a sign ambiguity fixed by the choice of  $\alpha_a$ . Thus, there are eight solutions of the PDE (10):

$$W^{(\alpha_1, \alpha_2, \alpha_3)}(\vec{\lambda}) = \sum_{a=1}^3 (-1)^{\alpha_a} \frac{1}{3} (\lambda_a + 2) \sqrt{1 - \lambda_a} \quad (12)$$

The generalization of equation (9) to the  $N$ -component scalar field case is solved using the same ansatz:  $W = \sum_{a=1}^N W_a$  leads us to the solution:  $W^{(\alpha_1, \dots, \alpha_N)}(\vec{\lambda}) = \sum_{a=1}^N (-1)^{\alpha_a} \frac{1}{3} (\lambda_a + 2) \sqrt{1 - \lambda_a}$ .

The energy for static configurations is written in elliptic coordinates as:

$$E[\vec{\lambda}] = \frac{m^3}{2\lambda^2\sqrt{2}} \int dx \sum_{a,b=1}^3 \left\{ g_{ab}(\vec{\lambda}) \frac{d\lambda_a}{dx} \cdot \frac{d\lambda_b}{dx} + g_{ab}^{-1}(\vec{\lambda}) \frac{\partial W^{(\alpha_1, \alpha_2, \alpha_3)}}{\partial \lambda_a} \frac{\partial W^{(\alpha_1, \alpha_2, \alpha_3)}}{\partial \lambda_b} \right\} \quad (13)$$

The possibility of writing the potential energy as a “square” in this way means that the (1+1)-dimensional field theory system admits a  $N = 1$  super-symmetric extension. Here we shall not discuss the super-symmetric system; instead, we focus on the fact that the energy can be written à la Bogomolny [2]:

$$\begin{aligned} E[\vec{\lambda}] &= \frac{m^3}{2\lambda^2\sqrt{2}} \left[ \int dx \sum_{a,b=1}^3 g_{ab}(\vec{\lambda}) \left[ \frac{d\lambda_a}{dx} + \sum_{c=1}^3 g_{ac}^{-1}(\vec{\lambda}) \frac{\partial W^{(\alpha_1, \alpha_2, \alpha_3)}}{\partial \lambda_c} \right] \left[ \frac{d\lambda_b}{dx} + \sum_{d=1}^3 g_{bd}^{-1}(\vec{\lambda}) \frac{\partial W^{(\alpha_1, \alpha_2, \alpha_3)}}{\partial \lambda_d} \right] \right] \\ &+ \frac{m^3}{\lambda^2\sqrt{2}} \left[ \int dx \sum_{a=1}^3 \frac{\partial W^{(\alpha_1, \alpha_2, \alpha_3)}}{\partial \lambda_a} [\vec{\lambda}] \frac{d\lambda_a}{dx} \right] \end{aligned} \quad (14)$$

The first integral in (14) gives a semi-definite positive contribution and there is a bound to the energy of a kink that satisfies the inequality:  $E[\vec{\lambda}] \geq \frac{m^3}{\lambda^2\sqrt{2}} \left| \int_P \sum_{a=1}^3 \frac{\partial W^{(\alpha_1, \alpha_2, \alpha_3)}}{\partial \lambda_a} [\vec{\lambda}] d\lambda_a \right|$ . The Bogomolny bound is saturated -the inequality becomes equality- if the “first-order” equations

$$\begin{aligned} \frac{d\lambda_1}{dx} &= (-1)^{\alpha_1} 2 \frac{\lambda_1(\lambda_1 - \bar{\sigma}_2^2)(\lambda_1 - \bar{\sigma}_3^2)}{(\lambda_1 - \lambda_2)(\lambda_1 - \lambda_3)} \cdot \sqrt{1 - \lambda_1} \\ \frac{d\lambda_2}{dx} &= (-1)^{\alpha_2} 2 \frac{\lambda_2(\lambda_2 - \bar{\sigma}_2^2)(\lambda_2 - \bar{\sigma}_3^2)}{(\lambda_2 - \lambda_1)(\lambda_2 - \lambda_3)} \cdot \sqrt{1 - \lambda_2} \\ \frac{d\lambda_3}{dx} &= (-1)^{\alpha_3} 2 \frac{\lambda_3(\lambda_3 - \bar{\sigma}_2^2)(\lambda_3 - \bar{\sigma}_3^2)}{(\lambda_3 - \lambda_1)(\lambda_3 - \lambda_2)} \cdot \sqrt{1 - \lambda_3} \end{aligned} \quad (15)$$

are satisfied. We see that the existence of eight superpotentials is related to the choice of signs in the right members of the ODE system (15). Alternatively, we could fix the superpotential, e.g. by setting  $\alpha_1 = \alpha_2 = \alpha_3 = 0$ , and allow for an independent choice of signs in each equation in (15) or in the Bogomolny splitting (14). In any case, (15) constitutes eight different systems of three ordinary differential equations.

We write the system (15) in the form:

$$\frac{d\lambda_a}{(-1)^{\alpha_a} 2\lambda_a(\lambda_a - \bar{\sigma}_2^2)(\lambda_a - \bar{\sigma}_3^2)\sqrt{1 - \lambda_a}} = \frac{dx}{f_a(\vec{\lambda})}; \quad a = 1, 2, 3 \quad (16)$$

The sum of the three equations in (16) reads:

$$\sum_{a=1}^3 \frac{d\lambda_a}{(-1)^{\alpha_a} 2\lambda_a(\lambda_a - \bar{\sigma}_2^2)(\lambda_a - \bar{\sigma}_3^2)\sqrt{1 - \lambda_a}} = 0 \quad (17)$$

We can also re-organize the equation (16) multiplying both members by  $\lambda_a - \lambda_b$ ,  $a \neq b$ . Thus, this equivalent form of the ODE system (16) contains six equations that can be added to obtain:

$$\sum_{a=1}^3 \frac{\lambda_a d\lambda_a}{(-1)^{\alpha_a} 2\lambda_a(\lambda_a - \bar{\sigma}_2^2)(\lambda_a - \bar{\sigma}_3^2)\sqrt{1 - \lambda_a}} = 0, \quad (18)$$



through the use of the three equations in (16). Integration of (17) and (18) provides all the separatrix orbits of the mechanical analogue system obtained by means of the Hamilton-Jacobi principle applied for zero particle energy and zero separation constants: compare with equations (31) and (32) for  $N = 3$  in Reference [1]. Therefore, all the orbits found there are the kink solutions of the first-order system (15). The kink form factors -the kink trajectories in the dynamical system terminology- are obtained after multiplication of the three equations in (16) by  $f_a(\vec{\lambda})$ , addition of the three resulting identities, and use of (17) and (18):

$$\sum_{a=1}^3 \frac{\lambda_a^2 d\lambda_a}{(-1)^{\alpha_a} 2\lambda_a(\lambda_a - \bar{\sigma}_2^2)(\lambda_a - \bar{\sigma}_3^2)\sqrt{1 - \lambda_a}} = dx, \quad (19)$$

Note that the boundary conditions (5) in elliptic coordinates read:

$$\lim_{x \rightarrow \pm\infty} \frac{d\lambda_a}{dx} = 0, \quad \lim_{x \rightarrow \pm\infty} \lambda_1(x) = 0, \quad \lim_{x \rightarrow \pm\infty} \lambda_2(x) = \bar{\sigma}_3^2, \quad \lim_{x \rightarrow \pm\infty} \lambda_3(x) = \bar{\sigma}_2^2. \quad (20)$$

Moreover, by squaring the first equation in (15) and defining the generalized momentum  $\pi_1 = g_{11}(\vec{\lambda}) \frac{d\lambda_1}{dx}$ , we obtain:

$$\frac{1}{2}\pi_1^2 + \frac{1}{8} \frac{\lambda_1^2}{\lambda_1 - 1} = 0 \quad (21)$$

Equation (21) describes the motion of a particle with zero energy moving under the influence of a potential

$$\begin{aligned} \mathcal{U}(\lambda_1) &= \frac{1}{4} \frac{\lambda_1^2}{\lambda_1 - 1}, & -\infty < \lambda_1 \leq \bar{\sigma}_3^2 \\ &= \infty, & \bar{\sigma}_3^2 < \lambda_1 < \infty \end{aligned}$$

$\mathcal{U}(\lambda_1)$  has a maximum at  $\lambda_1 = 0$  and goes to  $-\infty$  when  $\lambda_1$  tends to  $-\infty$ ; therefore, bounded motion occurs only in the  $\lambda_1 \in [0, \bar{\sigma}_3^2]$  interval. Together with the boundary conditions (20), this means that the kink configurations lie in the finite parallelepiped  $\bar{\mathbf{P}}_3(0)$ :  $0 \leq \lambda_1 \leq \bar{\sigma}_3^2 \leq \lambda_2 \leq \bar{\sigma}_2^2 \leq \lambda_3 \leq 1$ .

## 2.3 Kink solutions and Kink energies

In this section we shall analyze the solutions of the first order equations (15). The change in coordinates from Cartesian to elliptic is singular at each face in  $\bar{\mathbf{P}}_3(0)$ , except at the dynamical frontier  $\lambda_1 = 0$ . We shall thus deal carefully with the limiting behaviour of the system in  $\partial\bar{\mathbf{P}}_3(0)$ . There is a dimensional reduction of the system at these points and we expect a different kind of behaviour with respect to the regular points of the interior of  $\bar{\mathbf{P}}_3(0)$ . Computation of the energies of the kink solutions can be performed by noticing that the solutions of the first-order equations (15) saturate the Bogomolny bound:  $E[\vec{\lambda}_K] = \left| \int_K dW^{(\alpha_1, \alpha_2, \alpha_3)} \right|$

### 2.3.1 Generic Kinks.

Integration of (17) and (18) provides the orbits that the generic kinks trace in the internal space  $\mathbb{R}^3$ :

$$\sum_{a=1}^3 \frac{(-1)^{\alpha_a}}{2} \int \frac{d\lambda_a}{\lambda_a(\lambda_a - \bar{\sigma}_2^2)(\lambda_a - \bar{\sigma}_3^2)\sqrt{1 - \lambda_a}} = \gamma_2 \quad (22)$$

$$\sum_{a=1}^3 \frac{(-1)^{\alpha_a}}{2} \int \frac{\lambda_a d\lambda_a}{\lambda_a(\lambda_a - \bar{\sigma}_2^2)(\lambda_a - \bar{\sigma}_3^2)\sqrt{1 - \lambda_a}} = \gamma_3, \quad (23)$$

where  $\gamma_2$  and  $\gamma_3$  are real integration constants. The kink form factor is obtained from integration of the equation (19),

$$\sum_{a=1}^3 \frac{(-1)^{\alpha_a}}{2} \int \frac{\lambda_a^2 d\lambda_a}{\lambda_a(\lambda_a - \bar{\sigma}_2^2)(\lambda_a - \bar{\sigma}_3^2)\sqrt{1 - \lambda_a}} = \gamma_1 + x, \quad (24)$$

and depends on a third integration constant  $\gamma_1$ . Thus, the solitary kink waves of our system are composed of two ingredients: the orbit and the form factor.

The explicit integrations in (22) and (23) are performed in Reference [1], where they are written in compact form in formulas (35) and (36). All the TK3 kink orbits found there are described in sub-Section §3.2 of [1] by means of a numerical algorithm implemented in Mathematica (here we reproduce Figure 1 of a generic TK3 in both Cartesian and elliptic space). We refer the reader to that paper for information about the TK3 curves.

Instead, we now focus on computing the energy of a TK3 generic kink as a Bogomolny bound: generic TK3 orbits grow from several steps, according to the different choices of signs in equations (17)-(18). Each piece of any TK3 orbit is a solution of the equations (17)-(18), such that on these curves the TK3 kink also complies with (19). The signs in each stage, i.e., the values of  $\alpha_a$  in the equations (17)-(18)-(19), must be chosen according to the sense of change in the elliptic variables along the corresponding piece of orbit.

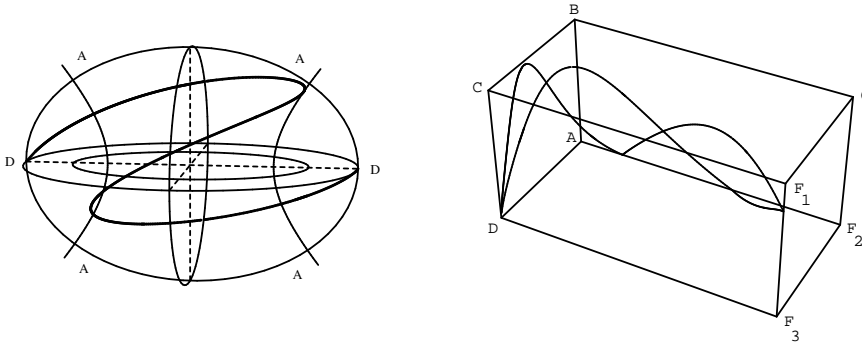


Figure 1: Orbit of a TK3 in  $\mathbb{R}^3$  and  $\bar{\mathbf{P}}_3(0)$ .

The behaviour of a generic TK3 solution in  $\bar{\mathbf{P}}_3(0)$  is as follows:

- 1. Starting from the point D, with coordinates in  $\bar{\mathbf{P}}_3(0)$ :  $D \equiv (0, \bar{\sigma}_3^2, \bar{\sigma}_2^2)$  at  $x \rightarrow -\infty$ , the first step travels in  $\mathbf{P}_3(0)$  to a point that we shall denote as  $P_1$ , the intersection of the kink with the face  $\lambda_3 = 1$  in  $\partial\mathbf{P}_3(0)$ , attained for some  $x = x_1$  (note that the invariance under translations in  $x$ , i.e., the arbitrariness of fixing  $\gamma_1$ , makes the exact value of  $x_1$  arbitrary too). The coordinates of  $P_1$  will be  $P_1 \equiv (\lambda_1^{P_1}, \lambda_2^{P_1}, 1)$ , and hence for  $x \in (-\infty, x_1]$  we have that  $\lambda_1, \lambda_2$  and  $\lambda_3$  increase. Thus,  $\frac{d\lambda_1}{dx}, \frac{d\lambda_2}{dx}$  and  $\frac{d\lambda_3}{dx}$  are positive for this range and we may conclude that from D to  $P_1$  the first-order equations (15) are satisfied if we consider  $\alpha_1 = \alpha_2 = \alpha_3 = 0$  in the choice of the super-potential  $W^{(\alpha_1, \alpha_2, \alpha_3)}$ .

- 2. In the second step, the TK3 returns to the interior of the parallelepiped,  $\mathbf{P}_3(0)$ , finishing at point  $P_2$ , the intersection with the edge  $AF_2$ . The coordinates of  $P_2$  are  $P_2 \equiv (\lambda_1^{P_2}, \bar{\sigma}_2^2, \bar{\sigma}_2^2)$  and this is reached for a value  $x = x_2 > x_1$ . In a similar way to the analysis performed for the first step, we have that for  $x \in (x_1, x_2]$ , i.e. from  $P_1$  to  $P_2$ , equations (15) are satisfied only if we consider the super-potential  $W^{(0,0,1)}$ .
- 3. In the third step, the kink travels from the  $AF_2$  edge to the  $F_1F_3$  one, which is reached at point  $P_3 \equiv (\bar{\sigma}_3^2, \bar{\sigma}_3^2, \lambda_3^{P_3})$  when  $x = x_3$ . The behaviour of the variables impose the super-potential  $W^{(0,1,0)}$  in equations (15).
- 4. From  $P_3$  to  $P_4$ , again in the face  $\lambda_3 = 1$ , we obtain the super-potential  $W^{(1,0,0)}$ .
- 5. In step 5, we find a similar situation to step 2, but the variable  $\lambda_1$  decreases, and hence we need  $W^{(1,0,1)}$  from  $P_4$  to  $P_5$ .
- 6. Denoting the third crossing of the  $\lambda_3 = 1$  face of  $\partial\mathbf{P}_3(0)$  as  $P_6$ , we have that from  $P_5$  to  $P_6$  the correct super-potential to be considered is  $W^{(1,1,0)}$ .
- 7. Finally, from  $P_6$  to point D we reproduce the first step in the opposite order, for the interval  $x \in (x_6, \infty)$ .

With all these considerations, the energy can be computed, step by step, as follows:

$$\begin{aligned}
\frac{\lambda^2\sqrt{2}}{m^3} E(\text{TK3}) &= - \int_{\text{TK3}} dW^{(\alpha_1, \alpha_2, \alpha_3)} = - \int_D^{P_1} dW^{(0,0,0)} - \int_{P_1}^{P_2} dW^{(0,0,1)} - \int_{P_2}^{P_3} dW^{(0,1,0)} \\
&\quad - \int_{P_3}^{P_4} dW^{(1,0,0)} - \int_{P_4}^{P_5} dW^{(1,0,1)} - \int_{P_5}^{P_6} dW^{(1,1,0)} - \int_{P_6}^D dW^{(1,1,1)} \\
&= \frac{4}{3} + \frac{2}{3} [\sigma_2(3 - \sigma_2^2) + \sigma_3(3 - \sigma_3^2)]
\end{aligned}$$

For instance,

$$\begin{aligned}
\int_D^{P_1} dW^{(0,0,0)} &= \int_0^{\lambda_1^{P_1}} \frac{\lambda_1 d\lambda_1}{2\sqrt{1-\lambda_1}} + \int_{\bar{\sigma}_3^2}^{\lambda_2^{P_1}} \frac{\lambda_2 d\lambda_2}{2\sqrt{1-\lambda_2}} + \int_{\bar{\sigma}_2^2}^1 \frac{\lambda_3 d\lambda_3}{2\sqrt{1-\lambda_3}} \\
\int_{P_1}^{P_2} dW^{(0,0,1)} &= \int_{\lambda_1^{P_1}}^{\lambda_1^{P_2}} \frac{\lambda_1 d\lambda_1}{2\sqrt{1-\lambda_1}} + \int_{\lambda_2^{P_1}}^{\bar{\sigma}_2^2} \frac{\lambda_2 d\lambda_2}{2\sqrt{1-\lambda_2}} - \int_1^{\bar{\sigma}_2^2} \frac{\lambda_3 d\lambda_3}{2\sqrt{1-\lambda_3}},
\end{aligned}$$

and so on. It is easy to convince oneself that the sum is independent of the coordinates  $\lambda_i^{P_j}$  of the concrete intersection points  $P_j$  and we see that  $E(\text{TK3})$  is the same for all the TK3 kinks. The TK3 kink energy is not a topological quantity because it depends on  $W_1^{(\alpha_1)}(\bar{\sigma}_3^2)$ ,  $W_2^{(\alpha_2)}(\bar{\sigma}_2^2)$ ,  $W_3^{(\alpha_3)}(1)$ , and not only on the value of  $W^{(\alpha_1, \alpha_2, \alpha_3)}$  at D:  $W_1^{(\alpha_1)}(0)$ ,  $W_2^{(\alpha_2)}(\bar{\sigma}_3^2)$ ,  $W_3^{(\alpha_3)}(\bar{\sigma}_2^2)$ .

### 2.3.2 Enveloping Kinks.

At the  $\lambda_1 = 0$  face, the ellipsoid  $\phi_1^2 + \frac{\phi_2^2}{\sigma_2^2} + \frac{\phi_3^2}{\sigma_3^2} = 1$  in  $\mathbb{R}^3$ , we note that the super-potential reduces to:

$$W^{(\alpha_1, \alpha_2)}(\vec{\mu}) = \frac{1}{3} \left( (-1)^{\alpha_1} (\mu_1 + 2) \sqrt{1 - \mu_1} + (-1)^{\alpha_2} (\mu_2 + 2) \sqrt{1 - \mu_2} \right) \quad (25)$$

Here, we denote by  $\lambda_2 = \mu_1$ ,  $\lambda_3 = \mu_2$  the components of the two-vector  $\vec{\mu} = (\mu_1, \mu_2)$  that parametrizes the parallelogram  $\bar{\mathbf{P}}_2^\mu$ :  $\bar{\sigma}_3^2 \leq \mu_1 \leq \bar{\sigma}_2^2 \leq \mu_2 \leq 1$ . The reduction of the first-order equations for this two-dimensional system is:

$$\begin{aligned} \frac{d\mu_1}{dx} &= (-1)^{\alpha_1} 2 \frac{(\mu_1 - \bar{\sigma}_2^2)(\mu_1 - \bar{\sigma}_3^2)}{(\mu_1 - \mu_2)} \cdot \sqrt{1 - \mu_1} \\ \frac{d\mu_2}{dx} &= (-1)^{\alpha_2} 2 \frac{(\mu_2 - \bar{\sigma}_2^2)(\mu_2 - \bar{\sigma}_3^2)}{(\mu_2 - \mu_1)} \cdot \sqrt{1 - \mu_2} \end{aligned} \quad (26)$$

Arguing in a similar vein to that developed in sub-section §2.2, we find that kinks living on the face  $\lambda_1 = 0$  satisfy the equation:

$$\sum_{a=1}^2 \frac{d\mu_a}{(-1)^{\alpha_a} 2 (\mu_a - \bar{\sigma}_2^2)(\mu_a - \bar{\sigma}_3^2) \sqrt{1 - \mu_a}} = 0 \quad (27)$$

and have their form factor determined by:

$$\sum_{a=1}^2 \frac{\mu_a d\mu_a}{(-1)^{\alpha_a} 2 (\mu_a - \bar{\sigma}_2^2)(\mu_a - \bar{\sigma}_3^2) \sqrt{1 - \mu_a}} = dx. \quad (28)$$

The integration of equation (27) is explicitly shown in the formula (48) of Reference [1]. These orbits lie on the  $\lambda_1 = 0$  face of  $\bar{\mathbf{P}}_3(0)$  and are graphically represented in Figure 4 of [1]. Each member of the family is a non-topological kink with three non-null components in Cartesian coordinates. The NTK3 non-topological kinks are enveloping kinks in the sense that they live on the face of  $\partial\bar{\mathbf{P}}_3(0)$ ; beyond this face in  $\bar{\mathbf{P}}_3(\infty)$ , i.e. for  $\lambda_1 < 0$ , there are no kink orbits. The NTK3 kink form factors are obtained from the integration of (28):

$$\begin{aligned} \exp\{2(\gamma_1 + x)(\sigma_3^2 - \sigma_2^2)\sigma_2\sigma_3\} &= \left| \frac{\sqrt{1 - \lambda_2} - \sigma_2}{\sqrt{1 - \lambda_2} + \sigma_2} \right|^{\sigma_3 \bar{\sigma}_2^2 (-1)^\alpha} \cdot \left| \frac{\sqrt{1 - \lambda_2} + \sigma_3}{\sqrt{1 - \lambda_2} - \sigma_3} \right|^{\sigma_2 \bar{\sigma}_3^2 (-1)^\alpha} \\ &\quad \cdot \left| \frac{\sqrt{1 - \lambda_3} - \sigma_2}{\sqrt{1 - \lambda_3} + \sigma_2} \right|^{\sigma_3 \bar{\sigma}_2^2 (-1)^\beta} \cdot \left| \frac{\sqrt{1 - \lambda_3} + \sigma_3}{\sqrt{1 - \lambda_3} - \sigma_3} \right|^{\sigma_2 \bar{\sigma}_3^2 (-1)^\beta} \end{aligned} \quad (29)$$

A NTK3 solution starts at  $x \rightarrow -\infty$  at the vacuum point  $D \equiv (\bar{\sigma}_3^2, \bar{\sigma}_2^2) \in \bar{\mathbf{P}}_2^\mu$ , and goes to the  $\mu_2 = 1$  edge, which is crossed, at  $x = x_1$ , at point  $P_1$ . It is thus necessary that both  $\frac{d\mu_1}{dx}$  and  $\frac{d\mu_2}{dx}$  should be positive in the  $D \rightarrow P_1$  step, and hence  $\alpha_1$  and  $\alpha_2$ , by (26), are both 0 in this situation.

From  $x_1$  to  $x_2$ , the kink continues its journey to arrive at the umbilicus A, with coordinates  $A \equiv (\bar{\sigma}_2^2, \bar{\sigma}_2^2)$ . Thus,  $\frac{d\mu_1}{dx}$  is positive and  $\frac{d\mu_2}{dx}$  is negative in the  $P_1 \rightarrow A$  step, and consequently

$\alpha_1 = 0$  and  $\alpha_2 = 1$ . The “return” from A to D is made in the opposite sense, with a new crossing of the BC edge at the point  $P_2$ . We thus have:  $A \rightarrow P_2$  ( $\alpha_1 = 1$  and  $\alpha_2 = 0$ ) and  $P_2 \rightarrow D$  ( $\alpha_1 = 1$  and  $\alpha_2 = 1$ ). We need to solve four different systems of first-order equations, continuously gluing the different pieces to describe a complete NTK3 kink. The energy is thus:

$$\begin{aligned} \frac{\lambda^2 \sqrt{2}}{m^3} E(\text{NTK3}) &= - \int_D^{P_1} d \left( W_1^{(0)} + W_2^{(0)} \right) - \int_{P_1}^A d \left( W_1^{(0)} + W_2^{(1)} \right) \\ &- \int_A^{P_2} d \left( W_1^{(1)} + W_2^{(0)} \right) - \int_{P_2}^D d \left( W_1^{(1)} + W_3^{(1)} \right) = 2 \left( \sigma_2 - \frac{\sigma_3^2}{3} \right) + 2 \left( \sigma_3 - \frac{\sigma_3^2}{3} \right) \end{aligned} \quad (30)$$

Obviously  $E(\text{NTK3})$  does not depend on the particular intersection points  $P_1$  and  $P_2$ , and hence the result is the same for all the kinks in the family. The NTK3 energy is not a topological quantity, however, because it depends on the value of  $W$  at the umbilicus point.

### 2.3.3 Embedded non-topological Kinks.

The system can be reduced to the  $N = 2$  MSTB model twice: in the  $\phi_3 = 0$ -plane and in the  $\phi_2 = 0$ -plane. Therefore, all the NTK2 kinks of the  $N = 2$  model are embedded in both planes.

The reduction of the system to the  $\phi_3 = 0$ -plane in  $\mathbb{R}^3$  occurs in two different faces of  $\bar{\mathbf{P}}_3(0)$ :  $\lambda_1 = \bar{\sigma}_3^2$  and  $\lambda_2 = \bar{\sigma}_2^2$ . We shall denote respectively by  $\bar{\mathbf{P}}_2^{\nu^I}(\bar{\sigma}_3^2, \bar{\sigma}_2^2)$  and  $\bar{\mathbf{P}}_2^{\nu^{II}}(0, \bar{\sigma}_2^2)$  the corresponding parallelograms:

$$\begin{aligned} \bar{\mathbf{P}}_2^{\nu^I}(\bar{\sigma}_3^2, \bar{\sigma}_2^2): & \bar{\sigma}_3^2 \leq \nu_1^I \leq \bar{\sigma}_2^2 \leq \nu_2^I \leq 1, \text{ with } \lambda_1 = \bar{\sigma}_3^2; \lambda_2 = \nu_1^I, \lambda_3 = \nu_2^I, \vec{\nu}^I = (\nu_1^I, \nu_1^I) \\ \bar{\mathbf{P}}_2^{\nu^{II}}(0, \bar{\sigma}_2^2): & 0 \leq \nu_1^{II} \leq \bar{\sigma}_3^2, \bar{\sigma}_2^2 \leq \nu_2^{II} \leq 1, \text{ with } \lambda_2 = \bar{\sigma}_3^2; \lambda_1 = \nu_1^{II}, \lambda_3 = \nu_2^{II}, \vec{\nu}^{II} = (\nu_1^{II}, \nu_1^{II}) \end{aligned}$$

The reduced super-potential is:

$$W^{(\alpha_1, \alpha_2)}(\vec{\nu}^{I, II}) = \frac{1}{3} \left( (-1)^{\alpha_1} (\nu_1^{I, II} + 2) \sqrt{1 - \nu_1^{I, II}} + (-1)^{\alpha_2} (\nu_2^{I, II} + 2) \sqrt{1 - \nu_2^{I, II}} \right) \quad (31)$$

and the first-order equations in both cases read:

$$\begin{aligned} \frac{d\nu_1^{I, II}}{dx} &= (-1)^{\alpha_1} 2 \frac{\nu_1^{I, II} (\nu_1^{I, II} - \bar{\sigma}_2^2)}{(\nu_1^{I, II} - \nu_2^{I, II})} \cdot \sqrt{1 - \nu_1^{I, II}} \\ \frac{d\nu_2^{I, II}}{dx} &= (-1)^{\alpha_2} 2 \frac{\nu_2^{I, II} (\nu_2^{I, II} - \bar{\sigma}_2^2)}{(\nu_2^{I, II} - \nu_1^{I, II})} \cdot \sqrt{1 - \nu_2^{I, II}} \end{aligned} \quad (32)$$

Analysis of a generic  $\text{NTK}2\sigma_2$  reveals to us the existence of six different pieces in an  $\text{NTK}2\sigma_2$  orbit. We only write the final result

$$\begin{aligned} \frac{\lambda^2 \sqrt{2}}{m^3} E(\text{NTK}2\sigma_2) &= - \int_{\text{NTK}2\sigma_2} d(W^{(\alpha_1, \alpha_2, \alpha_3)}) = - \int_D^{P_1} dW^{(0,0)}(\vec{\nu}^{II}) - \int_{P_1}^{P_2} dW^{(0,1)}(\vec{\nu}^{II}) \\ &- \int_{P_2}^{F_2} dW^{(0,1)}(\vec{\nu}^I) - \int_{F_2}^{P_3} dW^{(1,0)}(\vec{\nu}^I) - \int_{P_3}^{P_4} dW^{(1,0)}(\vec{\nu}^{II}) - \int_{P_4}^D dW^{(1,1)}(\vec{\nu}^{II}) = \frac{4}{3} + 2\sigma_2(1 - \frac{\sigma_2^2}{3}) \end{aligned}$$

and it is easy to reproduce the study in the  $\phi_2 = 0$ -plane, where we will obtain the energy of the  $\text{NTK}2\sigma_3$  family:  $\frac{\lambda^2 \sqrt{2}}{m^3} E(\text{NTK}2\sigma_3) = \frac{4}{3} + 2\sigma_3(1 - \frac{\sigma_3^2}{3})$ .

### 2.3.4 Embedded topological Kinks

Besides the NTK2 $\sigma_2$  and NTK2 $\sigma_3$  families, there are three more embedded kinks from the  $N = 2$  models, which are topological:

- TK1. The kink on the  $\phi_1$  axis in  $\mathbb{R}^3$  is a three-step orbit running on the edges DF<sub>3</sub>, F<sub>3</sub>F<sub>2</sub>, F<sub>2</sub>O and back to D through the same path. Equations (15) and their solutions, centered at the origin, in the three steps are:

1.  $\lambda_2 = \bar{\sigma}_3^2$  and  $\lambda_3 = \bar{\sigma}_2^2$ .  $\frac{d\lambda_1}{dx} = \pm 2\lambda_1\sqrt{1-\lambda_1}$ ,  $x \in (-\infty, -\arctanh \sigma_3] \sqcup [\arctanh \sigma_3, \infty)$ .  
 $\lambda_1^{\text{TK1}}(x) = 1 - \tanh^2 x$ ,  $\lambda_2^{\text{TK1}}(x) = \bar{\sigma}_3^2$ ,  $\lambda_3^{\text{TK1}}(x) = \bar{\sigma}_2^2$

2.  $\lambda_1 = \bar{\sigma}_3^2$  and  $\lambda_3 = \bar{\sigma}_2^2$ .  $\frac{d\lambda_2}{dx} = \pm 2\lambda_2\sqrt{1-\lambda_2}$ ,  $x \in [-\arctanh \sigma_3, -\arctanh \sigma_2] \sqcup [\arctanh \sigma_2, \arctanh \sigma_3]$ .  $\lambda_1^{\text{TK1}}(x) = \bar{\sigma}_3^2$ ,  $\lambda_2^{\text{TK1}}(x) = 1 - \tanh^2 x$ ,  $\lambda_3^{\text{TK1}}(x) = \bar{\sigma}_2^2$

3.  $\lambda_1 = \bar{\sigma}_3^2$  and  $\lambda_2 = \bar{\sigma}_2^2$ .  $\frac{d\lambda_3}{dx} = \pm 2\lambda_3\sqrt{1-\lambda_3}$ ,  $x \in [-\arctanh \sigma_2, 0] \sqcup [0, \arctanh \sigma_2]$ .  
 $\lambda_1^{\text{TK1}}(x) = \bar{\sigma}_3^2$ ,  $\lambda_2^{\text{TK1}}(x) = \bar{\sigma}_2^2$ ,  $\lambda_3^{\text{TK1}}(x) = 1 - \tanh^2 x$

The TK1 kinks are solutions of six different first-order equations in the intervals:  $x \in (\mp\infty, \mp\arctanh \sigma_3]$ ,  $x \in [\mp\arctanh \sigma_3, \mp\arctanh \sigma_2]$  and  $x \in [\mp\arctanh \sigma_2, 0]$ .

$E(\text{TK1}) = \frac{4m^3}{3\lambda^2\sqrt{2}}$  is not a topological quantity:

$$\frac{\lambda^2\sqrt{2}}{m^3} E(\text{TK1}) = - \int_{\text{D}}^{\text{F}_3} dW_1^{(0)} - \int_{\text{F}_3}^{\text{F}_2} dW_2^{(0)} - \int_{\text{F}_2}^{\text{O}} dW_3^{(0)} - \int_{\text{O}}^{\text{F}_2} dW_3^{(1)} - \int_{\text{F}_2}^{\text{F}_3} dW_2^{(1)} - \int_{\text{F}_3}^{\text{D}} dW_1^{(1)}$$

- The TK2 $\sigma_3$  kink. The restriction to the ellipse  $\phi_2 = 0$ ,  $\phi_1^2 + \frac{\phi_3^2}{\bar{\sigma}_3^2} = 1$  corresponds in  $\bar{\mathbf{P}}_3(0)$  to two edges of  $\partial\bar{\mathbf{P}}_3(0)$ : DA and AB.

At the DA edge,  $\lambda_1 = 0$  and  $\lambda_3 = \bar{\sigma}_2^2$ , the system (26) reduces to:

$$\frac{d\lambda_2}{dx} = \pm 2(\lambda_2 - \bar{\sigma}_3^2)\sqrt{1-\lambda_2} \quad (33)$$

with the solution, centered at the origin  $x_0 = 0$ :

$$\lambda_1^{\text{TK2}\sigma_3}(x) = 0, \quad \lambda_2^{\text{TK2}\sigma_3}(x) = 1 - \sigma_3^2 \tanh^2(\sigma_3 x), \quad \lambda_3^{\text{TK2}\sigma_3}(x) = \bar{\sigma}_2^2 \quad (34)$$

for  $x \in (-\infty, \frac{-1}{\sigma_3} \arctanh \frac{\sigma_2}{\sigma_3}] \sqcup [\frac{1}{\sigma_3} \arctanh \frac{\sigma_2}{\sigma_3}, \infty)$ . In the second step, the AB edge, equations (26) again reduce to a single differential equation: if  $\lambda_1 = 0$  and  $\lambda_2 = \bar{\sigma}_2^2$ , then

$$\frac{d\lambda_3}{dx} = \pm 2(\lambda_3 - \bar{\sigma}_3^2)\sqrt{1-\lambda_3} \quad (35)$$

has the solution

$$\lambda_1^{\text{TK2}\sigma_3}(x) = 0, \quad \lambda_2^{\text{TK2}\sigma_3}(x) = \bar{\sigma}_2^2, \quad \lambda_3^{\text{TK2}\sigma_3}(x) = 1 - \sigma_3^2 \tanh^2(\sigma_3 x) \quad (36)$$

for  $x \in [\frac{-1}{\sigma_3} \arctanh \frac{\sigma_2}{\sigma_3}, \frac{1}{\sigma_3} \arctanh \frac{\sigma_2}{\sigma_3}]$ . The energy is thus:

$$\begin{aligned} \frac{\lambda^2\sqrt{2}}{m^3} E(\text{TK2}\sigma_3) &= \int_{\text{TK2}\sigma_3} d(W_2^{(\alpha_2)} + W_3^{(\alpha_3)}) = \\ &= - \int_{\text{D}}^{\text{A}} dW_2^{(0)} + \int_{\text{A}}^{\text{B}} dW_3^{(0)} + \int_{\text{B}}^{\text{A}} dW_3^{(1)} + \int_{\text{A}}^{\text{D}} dW_2^{(1)} = 2\sigma_3 \left(1 - \frac{\sigma_3^2}{3}\right) \end{aligned}$$

The two steps are continuously sewn at the umbilicus point  $A \equiv (0, \bar{\sigma}_2^2, \bar{\sigma}_2^2)$ . Note that the  $\text{TK}2\sigma_3$  kinks are solutions of four different first-order equations on the intervals  $x \in (\mp\infty, \frac{\mp 1}{\sigma_3} \text{arctanh} \frac{\sigma_2}{\sigma_3}]$  and  $x \in [\frac{\pm 1}{\sigma_3} \text{arctanh} \frac{\sigma_2}{\sigma_3}, \frac{\pm 1}{\sigma_3} \text{arctanh} \frac{\sigma_2}{\sigma_3}]$  glued at the umbilicus point A.  $E(\text{TK}2\sigma_3)$  is not a topological quantity.

- The  $\text{TK}2\sigma_2$  kink. The restriction to the DC edge,  $\lambda_1 = 0$  and  $\lambda_2 = \bar{\sigma}_3^2$ , corresponds, in  $\mathbb{R}^3$ , to the ellipse  $\phi_3 = 0$  and  $\phi_1^2 + \frac{\phi_2^2}{\bar{\sigma}_2^2} = 1$ . System (26) reduces to:

$$\frac{d\lambda_3}{dx} = (-1)^\beta (\lambda_3 - \bar{\sigma}_2^2) \sqrt{1 - \lambda_3}. \quad (37)$$

The kink form factor is thus,

$$\lambda_1^{\text{TK}2\sigma_2}(x) = 0, \quad \lambda_2^{\text{TK}2\sigma_2}(x) = \bar{\sigma}_3^2, \quad \lambda_3^{\text{TK}2\sigma_2}(x) = 1 - \bar{\sigma}_2^2 \tanh^2(\sigma_2 x)$$

and the energy reads:

$$\frac{\lambda^2 \sqrt{2}}{m^3} E(\text{TK}2\sigma_2) = - \int_{\text{TK}2\sigma_2} dW_3^{(\beta)} = - \left[ \int_D^C dW_3^{(0)} + \int_C^D dW_3^{(1)} \right] = 2\sigma_2 \left( 1 - \frac{\sigma_2^2}{3} \right)$$

Note that  $W_3^{(\beta)}(C) = 0, \forall \beta = 0, 1$ , and hence the energy of the  $\text{TK}2\sigma_2$  kink depends only on the value of  $W_3^{(0)}$  and  $W_3^{(1)}$  at the vacuum D.  $E(\text{TK}2\sigma_2)$  is thus a topological quantity and in consequence  $\text{TK}2\sigma_2$  is the absolute minimum of the functional  $E$ ; necessarily, the  $\text{TK}2\sigma_2$  kink is a stable solution.

The rest of the kinks analyzed are not absolute minima of  $E$ , although they could be local minima. We shall see in section §4 that this is not the case and that all of them are unstable critical curves of  $E$ . According to the usual classification between BPS and non-BPS solitary waves in supersymmetric theories, we have shown that the only BPS solution of the equations of the system is the  $\text{TK}2\sigma_2$  kink.

## 3 The moduli space of kinks

### 3.1 kink-energy sum rules

The energies of the different kinks that we have calculated in the previous section are related in several ways. By inspection, we see the energy of a generic  $\text{TK}3$  kink as the sum of the energies of embedded and enveloping kinks. There are four primary sum rules:

1)

$$\boxed{E(\text{TK}3) = E(\text{NTK}2\sigma_3) + E(\text{TK}2\sigma_2)} \quad (38)$$

2)

$$\boxed{E(\text{TK}3) = E(\text{NTK}2\sigma_2) + E(\text{TK}2\sigma_3)} \quad (39)$$

3)

$$\boxed{E(\text{TK}3) = E(\text{NTK}3) + E(\text{TK}1)} \quad (40)$$

4)

$$\boxed{E(\text{NTK3}) = E(\text{TK2}\sigma_3) + E(\text{TK2}\sigma_2)} \quad (41)$$

As a consequence, we also find:

$$E(\text{TK3}) = E(\text{TK1}) + E(\text{TK2}\sigma_2) + E(\text{TK2}\sigma_3) \quad (42)$$

The old kink-energy sum rules, already appearing in the  $N = 2$  model [8] [9] and involving only embedded kinks, are also satisfied:

$$E(\text{NTK2}\sigma_3) = E(\text{TK2}\sigma_3) + E(\text{TK1}); \quad E(\text{NTK2}\sigma_2) = E(\text{TK2}\sigma_2) + E(\text{TK1}). \quad (43)$$

### 3.2 The variety of kink trajectories: Singular limits

In this sub-section we shall show how the kink solutions of the dimensionally reduced equations are singular limits of the generic TK3 kinks obtained by letting  $\gamma_2$  and  $\gamma_3$  go to  $\pm\infty$  in formulae (35) and (36) of Reference [1]. This circumstance fully explains the origin of the kink-energy sum rules: suitable combinations of enveloping and embedded kinks arise at the boundary of the families of generic kinks.

In order to describe the process of reaching the singular limits in a complete way, it is convenient to look at the manifold of TK3 kinks as the set of solutions of a re-shuffling of the equations (17) and (18). Two equivalent equations are obtained through multiplication of (18); first by  $\bar{\sigma}_3^2$ , then by  $\bar{\sigma}_2^2$ , and subtraction of (17) from both expressions. The solutions to this equivalent system are:

$$\begin{aligned} e^{2\sigma_2\bar{\sigma}_2^2\gamma} &= \left( \left| \frac{\sqrt{1-\lambda_1}-1}{\sqrt{1-\lambda_1}+1} \right|^{\sigma_2} \cdot \left| \frac{\sqrt{1-\lambda_1}+\sigma_2}{\sqrt{1-\lambda_1}-\sigma_2} \right| \right)^{(-1)^{\alpha_1}} \cdot \\ &\quad \left( \left| \frac{\sqrt{1-\lambda_2}-1}{\sqrt{1-\lambda_2}+1} \right|^{\sigma_2} \cdot \left| \frac{\sqrt{1-\lambda_2}+\sigma_2}{\sqrt{1-\lambda_2}-\sigma_2} \right| \right)^{(-1)^{\alpha_2}} \cdot \\ &\quad \left( \left| \frac{\sqrt{1-\lambda_3}-1}{\sqrt{1-\lambda_3}+1} \right|^{\sigma_2} \cdot \left| \frac{\sqrt{1-\lambda_3}+\sigma_2}{\sqrt{1-\lambda_3}-\sigma_2} \right| \right)^{(-1)^{\alpha_3}} \end{aligned} \quad (44)$$

and

$$\begin{aligned} e^{2\sigma_3\bar{\sigma}_3^2\bar{\gamma}} &= \left( \left| \frac{\sqrt{1-\lambda_1}-1}{\sqrt{1-\lambda_1}+1} \right|^{\sigma_3} \cdot \left| \frac{\sqrt{1-\lambda_1}+\sigma_3}{\sqrt{1-\lambda_1}-\sigma_3} \right| \right)^{(-1)^{\alpha_1}} \cdot \\ &\quad \left( \left| \frac{\sqrt{1-\lambda_2}-1}{\sqrt{1-\lambda_2}+1} \right|^{\sigma_3} \cdot \left| \frac{\sqrt{1-\lambda_2}+\sigma_3}{\sqrt{1-\lambda_2}-\sigma_3} \right| \right)^{(-1)^{\alpha_2}} \cdot \\ &\quad \left( \left| \frac{\sqrt{1-\lambda_3}-1}{\sqrt{1-\lambda_3}+1} \right|^{\sigma_3} \cdot \left| \frac{\sqrt{1-\lambda_3}+\sigma_3}{\sqrt{1-\lambda_3}-\sigma_3} \right| \right)^{(-1)^{\alpha_3}} \end{aligned} \quad (45)$$

where the “new” integration constants are:  $\gamma = \gamma_3\bar{\sigma}_3^2 - \gamma_2$  and  $\bar{\gamma} = \gamma_3\bar{\sigma}_2^2 - \gamma_2$ .

All the generic kink orbits are described analytically by (44) and (45). The advantage of using  $\gamma$  and  $\bar{\gamma}$  in the parametrization of the TK3 family is the following: in terms of the constants  $\gamma$  and  $\bar{\gamma}$  one determines the intersection points of a generic TK3 orbit with the



edges of  $\bar{\mathbf{P}}_3(0)$   $\lambda_1 = \lambda_2 = \bar{\sigma}_3^2$ , the ellipse (63) in Cartesian coordinates, and  $\lambda_2 = \lambda_3 = \bar{\sigma}_2^2$ , the hyperbola (64), which are precisely the lines along which the super-potential is non-differentiable. If  $\tilde{\lambda}_3$  is a root of the equation:

$$e^{2\sigma_2\bar{\sigma}_2^2\gamma} = \left( \left| \frac{\sqrt{1-\tilde{\lambda}_3}-1}{\sqrt{1-\tilde{\lambda}_3}+1} \right|^{\sigma_2} \cdot \left| \frac{\sqrt{1-\tilde{\lambda}_3}+\sigma_2}{\sqrt{1-\tilde{\lambda}_3}-\sigma_2} \right| \right)^{(-1)\alpha_3} \quad (46)$$

the point  $(\lambda_1, \lambda_2, \lambda_3) = (\bar{\sigma}_3^2, \bar{\sigma}_3^2, \tilde{\lambda}_3)$  is the intersection point of the TK3 orbit with the edge  $F_1F_3$  in  $\bar{\mathbf{P}}_3(0)$  (the ellipse (63) in  $\mathbb{R}^3$ ). There are two  $\tilde{\lambda}_1^\pm$  roots of

$$e^{2\sigma_3\bar{\sigma}_3^2\bar{\gamma}} = \left( \left| \frac{\sqrt{1-\tilde{\lambda}_1}-1}{\sqrt{1-\tilde{\lambda}_1}+1} \right|^{\sigma_3} \cdot \left| \frac{\sqrt{1-\tilde{\lambda}_1}+\sigma_3}{\sqrt{1-\tilde{\lambda}_1}-\sigma_3} \right| \right)^{(-1)\alpha_1}, \quad (47)$$

depending on the choices of  $\alpha_1$ , which determine the two intersection points of the TK3 kink with the edge  $AF_2$  in  $\bar{\mathbf{P}}_3(0)$  (the hyperbola (64) in  $\mathbb{R}^3$ ). Thus, the analytical parametrization by  $(\gamma, \bar{\gamma})$  of the TK3 family acquires a geometric meaning. A choice of  $\bar{\gamma}$  fixes the intersection point of a given TK3 with the edge  $AF_2$ . There are, however, infinitely many TK3 orbits meeting at this point in  $AF_2$ ; this congruence comes from each point in  $F_1F_3$  and is parametrized by  $\gamma \in \mathbb{R}$ . Conversely, when  $\bar{\gamma}$  varies in  $\mathbb{R}$  a family of TK3 orbits is described that crosses every point in  $AF_2$  and meets at a single point at the edge  $F_1F_3$ , characterized by a fixed value of  $\gamma$ . The corresponding conics in  $\mathbb{R}^3$ , the ellipse (63), and the hyperbola (64) are lines where the gradient flow of the super-potential is undefined: a one-parameter family of TK3 orbits touching all points of the ellipse (63) meets at a single point of the hyperbola (64) and vice-versa.

It should be stressed that the boundary points A,  $F_1$ ,  $F_2$  and  $F_3$  are excluded because they are reached when either  $\gamma$  or  $\bar{\gamma}$  goes to  $\pm\infty$ , and for these values there are no generic kink orbits. The question arises: are there any kink orbits when  $\gamma$  or  $\bar{\gamma}$  are  $\pm\infty$ ?, or alternatively, when  $\gamma_2$  or  $\gamma_3$  are  $\pm\infty$ ? We shall show that this is indeed the case, at the same time justifying the kink-energy sum rules.

In the process of taking  $\gamma \rightarrow \pm\infty$  or  $\bar{\gamma} \rightarrow \infty$  (or the corresponding  $\gamma_2$  and/or  $\gamma_3 \rightarrow \pm\infty$ ) different singular solutions appear, depending on the choice of  $\alpha_1, \alpha_2$  and  $\alpha_3$  in equations (44) and (45). For instance, taking  $\gamma \rightarrow -\infty$  in (44) leads us to  $\lambda_1 \rightarrow 0$  if we consider  $\alpha_1 = 0$ , but it is also compatible with  $\lambda_2 \rightarrow \bar{\gamma}_2^2$  if  $\alpha_2 = 1$  with no restrictions to the value of  $\alpha_1$ , and so on. In Reference [7] the singular limits have been carefully explored, looking at all the combinations of the different signs allowed. We here summarize only the final results, because the very technical details add nothing further to our conceptual knowledge of the subject.

The five possible singular limits in the TK3 kink space are:

- $\gamma \rightarrow \pm\infty$ ,  $\bar{\gamma}$  finite. As one can check in Appendix A, taking  $\gamma \rightarrow \pm\infty$ ,  $\bar{\gamma}$  remaining finite, leads us, in a non-trivial way, to the combination of an NTK2 $\sigma_3$  (determined by the particular value of  $\bar{\gamma}$ ) plus the TK2 $\sigma_2$ . Later taking the  $\bar{\gamma} \rightarrow \pm\infty$  limit, one arrives at the combination of orbits TK2 $\sigma_3$ + TK2 $\sigma_2$ + TK1.
- $\bar{\gamma} \rightarrow \pm\infty$ , finite  $\gamma$ . In a similar way, it is possible to show that this limit is reached at the combination of one NTK2 $\sigma_2$  (parametrized by  $\gamma$ ) plus the TK2 $\sigma_3$  orbit. Later taking the  $\gamma \rightarrow \pm\infty$  limit leads to TK2 $\sigma_3$ + TK2 $\sigma_2$ + TK1.
- $\gamma_3 \rightarrow \pm\infty$ , finite  $\gamma_2$ . In this case, the result is an NTK3 orbit (determined by the value of  $\gamma_2$ ) plus the TK1 orbit. Later passing to the  $\gamma_2 \rightarrow \pm\infty$  limit produces the combination TK2 $\sigma_3$ + TK2 $\sigma_2$ + TK1.

- $\gamma_2 \rightarrow \pm\infty$ , finite  $\gamma_3$ . This situation is in some sense the most singular; regardless of the particular value of the constant  $\gamma_3$ , the limit is always the combination  $\text{TK}2\sigma_3 + \text{TK}2\sigma_2 + \text{TK}1$ .
- Any other possibility of going to infinity in the space of parameters of the TK3 family, without the restrictions detailed in the previous cases, leads to the “most singular” combination:  $\text{TK}2\sigma_3 + \text{TK}2\sigma_2 + \text{TK}1$ .

### 3.3 Moduli space structure

The moduli space of kinks is defined as the space of solitary wave solutions of the field equations modulo the action of the symmetry group  $G = \mathbb{Z}^{\times 3}$  of the system. The action of the group  $G$  on the different kinds of kinks advanced in the Introduction is now clear after the analysis of the solutions discussed in the previous Sections. The sub-space of “points” that are not fixed under the action of any non-trivial sub-group of  $G$  is formed precisely by the solutions of (44)-(45) for finite values of  $\gamma$  and  $\bar{\gamma}$ : at any point  $(\gamma, \bar{\gamma}) \in \mathbb{R}^2 - \partial\mathbb{R}^2$  there is associated a generic TK3 kink trajectory in elliptic coordinates that corresponds to eight TK3 kinks in Cartesian space. Therefore, the moduli space of TK3 kinks in the deformed linear  $O(3)$ -sigma model is the open plane parametrized by the  $(\gamma, \bar{\gamma})$  integration constants. The aim of this Section is to describe how the other kinks of the system enter this moduli space. Any “member” of the moduli space must have the same energy as any other. Thus, we expect that the other kinks enter the moduli space of TK3 kinks assembled in such a way that the kink-energy sum rules will be saturated.

The embedded topological and non-topological kinks and the NTK3 enveloping kinks live at the boundary of the TK3 moduli space  $\mathbb{R}^2$  and provide a compactification of this space. The kind of compactification depends on how one goes to infinity in  $\mathbb{R}^2$  and how one chooses a particular degeneration of one TK3 kink to a specific assembly of the other kinks. To simplify the cumbersome labeling, we shall denote the different kinds of kinks according to the following Table:

TK3	$T_3$
NTK3+TK1	$N_3 T_1$
NTK2 $\sigma_3$ +TK2 $\sigma_2$	$N_2^{\sigma_3} T_2^{\sigma_2}$
NTK2 $\sigma_2$ +TK2 $\sigma_3$	$N_2^{\sigma_2} T_2^{\sigma_3}$
TK2 $\sigma_2$ +TK2 $\sigma_3$ +TK1	$T_2^{\sigma_2} T_2^{\sigma_3} T_1$

Only three “paths” to infinity will be important in developing degenerate Morse theory for the configuration space:

- a) Taking the limits  $\Lambda \rightarrow \pm\infty$  in the family of straight lines  $\gamma = \Lambda$ ,  $\Lambda \in \mathbb{R}$ , the moduli space of  $N_2^{\sigma_3} T_2^{\sigma_2}$  singular kink configurations is found. The plane becomes an infinite cylinder through identification of the  $\Lambda = \pm\infty$  lines. Moreover, all the points in the  $\bar{\gamma} = \pm\infty$  circles give the same  $T_2^{\sigma_2} T_2^{\sigma_3} T_1$  configuration -skipping the path which reaches these circles as described in b)- and must be identified to a point. The addition of two  $N_2^{\sigma_3} T_2^{\sigma_2}$  families amounts to compactifying the TK3 moduli space to a  $S^2$  sphere:  $\bar{\mathcal{M}}_{T_3}^{(1)} = \mathcal{M}_{T_3} \sqcup 2\mathcal{M}_{N_2^{\sigma_3} T_2^{\sigma_2}} \cong S^2$ .

- b) The above behaves in exactly the same way when the  $\gamma = \Lambda$  are replaced by the  $\bar{\gamma} = \Lambda$  lines. The  $N_2^{\sigma_2}T_2^{\sigma_3}$  moduli space arises on the  $\Lambda = \pm\infty$  lines. The gluing of these two lines provides an infinite cylinder, and the identification of the two  $\gamma = \pm\infty$  circles at infinity to a point, the  $T_2^{\sigma_2}T_2^{\sigma_3}T_1$  configuration, leads to the two-sphere:  $\bar{\mathcal{M}}_{T_3}^{(2)} = \mathcal{M}_{T_3} \sqcup 2\mathcal{M}_{N_2^{\sigma_2}T_2^{\sigma_3}} \cong S^2$ . Here, we skip the path to the  $\gamma = \pm\infty$  circles described in a).
- c) The third interesting possibility is to take the  $\Lambda \rightarrow \pm\infty$  limit in the family of straight lines:  $\bar{\gamma} = \gamma - \Lambda$ . Note that  $\gamma_3 = \text{constant}$  on these lines. We find the  $N_3T_1$  moduli space on both limits and the identification of these two lines leads to a third infinite cylinder. Again, the  $\gamma_3 = \pm\infty$  circles must be identified because all their points are the  $T_2^{\sigma_2}T_2^{\sigma_3}T_1$  configuration, and hence:  $\bar{\mathcal{M}}_{T_3}^{(3)} = \mathcal{M}_{T_3} \sqcup 2\mathcal{M}_{N_3T_1} \cong S^2$ .

## 4 Kink Stability

Let  $\vec{\psi}(x)$  be a path in a Riemannian manifold  $(M^3, g)$ . Using the language of variational calculus, let us denote by  $\vec{\psi}(x, \xi)$ ,  $\xi \in (-\varepsilon, \varepsilon)$ , a proper variation of  $\vec{\psi}$  and let  $\dot{\vec{\psi}}(x, \xi)$ ,  $\vec{V}(x, \xi)$  be the vector fields

$$\dot{\vec{\psi}}(x, \xi) = \frac{\partial \vec{\psi}}{\partial x}(x, \xi) \quad , \quad \vec{V}(x, \xi) = \frac{\partial \vec{\psi}}{\partial \xi}(x, \xi) \quad .$$

The Hessian quadratic form, the second variation of the energy functional,

$$E[\vec{\psi}] = \int dx \left( \frac{1}{2} \left\langle \frac{d\vec{\psi}}{dx}, \frac{d\vec{\psi}}{dx} \right\rangle + U(\vec{\psi}) \right) \quad , \quad (48)$$

at a ‘‘critical point’’ - a kink solution  $\vec{\psi}_K$  for which the first variation of  $E[\vec{\psi}]$  is zero-, is

$$\mathcal{H} = \int_{\vec{\psi}_K} dx \left\langle \Delta \vec{V}, \vec{V} \right\rangle = \int_{\vec{\psi}_K} dx \left\langle -\frac{D^2 \vec{V}}{dx^2} - K_{\dot{\vec{\psi}}_K}(\vec{V}) + \nabla_{\vec{V}} \vec{\text{grad}}(U), \vec{V} \right\rangle \quad (49)$$

Here,  $\frac{D\vec{V}}{dx}$  is the covariant derivative along the kink orbit,  $K_{\dot{\vec{\psi}}_K}(\vec{V}) = R(\dot{\vec{\psi}}_K, \vec{V})\dot{\vec{\psi}}_K$  is the sectional curvature defined in terms of the curvature tensor  $R$  and  $\nabla_{\vec{V}} \vec{\text{grad}}(U)$  is the covariant derivative of  $\vec{\text{grad}}U$  in the direction of  $\vec{V}$ . In a local coordinate system in  $M^3$ , the differential operator  $\Delta$  reads

$$\Delta_b^a = -\frac{D^2}{dx^2} \delta_b^a - [K_{\dot{\vec{\psi}}_K}]_b^a + \mathcal{U}_b^a(\vec{\psi}_K)$$

$$\frac{DV^a}{dx} = \frac{dV^a}{dx} + \Gamma_{bc}^a(\vec{\psi}_K) \frac{d\psi_K^b}{dx} V^c, \quad [K_{\dot{\vec{\psi}}_K}]_b^a = R_{cbd}^a \dot{\psi}_K^c \psi_K^d, \quad \mathcal{U}_b^a(\vec{\psi}_K) = \frac{\partial^2 U}{\partial \psi_a \partial \psi^b}(\vec{\psi}_K) - \Gamma_{cb}^a \frac{\partial U}{\partial \psi_c}(\vec{\psi}_K)$$

We shall consider  $\vec{\psi}$  as the static scalar field either in Cartesian  $-\vec{\phi}(x)-$  or in elliptic  $-\vec{\lambda}(x)-$  coordinates. Therefore,  $M^3$  is the Euclidean  $\mathbb{R}^3$  space in the first case and  $\mathbf{P}_3(\infty)$  with the metric induced by the change of coordinates, see Section §2.2, in the later case. Either way, the stability of kink solutions against small deformations is encoded in the spectrum of  $\Delta$ .

## 4.1 Jacobi fields and the Jacobi Theory

Even without knowing the analytical expression of  $\Delta$ , we can state a general fact about its spectrum: if there exists a kink family  $\vec{\psi}_K = \vec{\psi}_K(x, \gamma)$  of critical points of  $E[\vec{\psi}]$  characterized by the value of the parameter  $\gamma$ , then the vector field  $\frac{\partial \vec{\psi}_K}{\partial \gamma}$  is a Jacobi field, i.e. it belongs to the kernel of  $\Delta$ ,

$$\left\langle \Delta \frac{\partial \vec{\psi}_K}{\partial \gamma}, \frac{\partial \vec{\psi}_K}{\partial \gamma} \right\rangle = \frac{\partial}{\partial \gamma} \left\langle -\frac{D}{\partial x} \vec{\psi}_K + \text{grad}U(\vec{\psi}_K), \frac{\partial \vec{\psi}_K}{\partial \gamma} \right\rangle - \left\langle -\frac{D}{\partial x} \vec{\psi}_K + \text{grad}U(\vec{\psi}_K), \frac{D}{\partial \gamma} \frac{\partial \vec{\psi}_K}{\partial \gamma} \right\rangle = 0$$

Any generic TK3 kink therefore gives rise to three Jacobi fields:  $\frac{\partial \vec{\psi}_{\text{TK3}}}{\partial \gamma_1}$  is tangent to the orbit and is usually termed as the translational mode.  $\frac{\partial \vec{\psi}_{\text{TK3}}}{\partial \gamma_2}$  and  $\frac{\partial \vec{\psi}_{\text{TK3}}}{\partial \gamma_3}$ , however, have non-zero components in the orthogonal sub-space to the trajectory in  $\mathcal{C}$  and obey zero ‘‘particle energy’’ fluctuations along the kink moduli space. Both the embedded and enveloping non-topological kinks form two-parametric families of solutions. Besides the translational mode, all of them present a second Jacobi field coming from the partial derivative of the field configuration with respect to the second integration constant.

According to the theory elaborated by Jacobi in the 19th century, see [11], Jacobi fields contain a lot of information about the stability of the trajectories to which they are associated. The application to our problem is as follows:

‘‘A kink trajectory is unstable if there is a non-trivial Jacobi field that vanishes at the endpoints of the real half-line:  $(-\infty, x_0]$ ’’. Essentially the argument is based on the following idea: the projection of  $\Delta$  in the direction of the Jacobi field is a Schrodinger operator. The Jacobi field itself belongs to the kernel of this operator but has at least one node: it cannot be the ground state. Therefore, the strategy to determine whether or not a kink orbit is stable is based on the study of the features of the Jacobi fields along these trajectories.

### 1. Non-topological kinks

We first focus on the **NTK** kinks. The three types can be described in a unified way by using the two-dimensional elliptic variables:  $c \leq \mu_1 \leq \bar{\sigma}^2 \leq \mu_2 \leq 1$ . Appropriate re-scalings and choices of the constants  $c$  and  $\bar{\sigma}^2$  lead to the elliptic coordinates which work for the NTK3, NTK2 $\sigma_3^2$ , and NTK2 $\sigma_2^2$  kinks. The kink orbit and the kink form factor are respectively determined by the equations:

$$\left( \left| \frac{\sqrt{1-\mu_1}-\sigma}{\sqrt{1-\mu_1}+\sigma} \right| \left| \frac{\sqrt{1-\mu_1}+1}{\sqrt{1-\mu_1}-1} \right|^\sigma \right)^{(-1)^{\alpha_1}} \left( \left| \frac{\sqrt{1-\mu_2}-\sigma}{\sqrt{1-\mu_2}+\sigma} \right| \left| \frac{\sqrt{1-\mu_2}+1}{\sqrt{1-\mu_2}-1} \right|^\sigma \right)^{(-1)^{\alpha_2}} = e^{2\sigma\bar{\sigma}^2\gamma_2} \quad (50)$$

$$\left| \frac{\sqrt{1-\mu_1}-\sigma}{\sqrt{1-\mu_1}+\sigma} \right|^{\bar{\sigma}^2(-1)^{\alpha_1}} \cdot \left| \frac{\sqrt{1-\mu_2}-\sigma}{\sqrt{1-\mu_2}+\sigma} \right|^{\bar{\sigma}^2(-1)^{\alpha_2}} = e^{2\sigma(x+\gamma_1)} \quad (51)$$

It is not possible to invert the system (50)-(51) and write  $\mu_1$  and  $\mu_2$  explicitly as elementary transcendental functions of  $x$ ; henceforth, one cannot explicitly write the Hessian operator for these configurations. To identify the orthogonal Jacobi field, however, we perform the implicit derivation of (50) and (51) with respect to  $\gamma_2$  and solve the linear system to find the components  $\frac{\partial \mu_1^{\text{NTK}}}{\partial \gamma_2}$ ,  $\frac{\partial \mu_2^{\text{NTK}}}{\partial \gamma_2}$  of the Jacobi field.

Before of doing so, we must first address a very subtle point: all the kink orbits - the solutions of (50)  $\forall \gamma_2$ - pass through the vacuum point ( $\bar{\mu}_1 = 0, \bar{\mu}_2 = \bar{\sigma}^2$ ) in the  $\alpha_1 = \alpha_2$  steps. There is only one other point crossed by all the kink orbits: the focus ( $\bar{\mu}_1 = \bar{\sigma}^2, \bar{\mu}_2 = \bar{\sigma}^2$ ) is reached by all the kink orbits in the  $\alpha_1 = 0, \alpha_2 = 1$  step and left in the  $\alpha_1 = 1, \alpha_2 = 0$  step. Note that the focus becomes the umbilicus point for the NTK3 kinks and the appropriate focus of the ellipsoid for the NTK2 $\sigma_2$  or NTK2 $\sigma_3$  kinks. Given a kink orbit ( $\bar{\mu}_1(x, \gamma_2), \bar{\mu}_2(x, \gamma_2)$ ), near the focus (50) becomes :

$$\lim_{(\bar{\mu}_1, \bar{\mu}_2) \rightarrow (\bar{\sigma}^2, \bar{\sigma}^2)} \frac{\sqrt{1 - \bar{\mu}_1} - \sigma}{\sqrt{1 - \bar{\mu}_2} - \sigma} = e^{\pm 2\sigma \bar{\sigma}^2 \gamma_2} \quad (52)$$

the +/- signs standing for the steps arriving at/departing from the focus. Taking the same limit in equation (51) and using (52), one immediately sees that the focus is reached at the “instant”  $x_0 = -\gamma_1 + \bar{\sigma}^4 \gamma_2$ . Here, the subtlety is: different kink trajectories reach the focus at different times.

Defining  $\bar{\gamma}_1 = \gamma_1 - \bar{\sigma}^4 \gamma_2$  equation (51) is replaced by the equivalent equation :

$$\left| \frac{\sqrt{1 - \mu_1} - 1}{\sqrt{1 - \mu_1} + 1} \right|^{\bar{\sigma}^2(-1)^{\alpha_1}} \cdot \left| \frac{\sqrt{1 - \mu_2} - 1}{\sqrt{1 - \mu_2} + 1} \right|^{\bar{\sigma}^2(-1)^{\alpha_2}} = e^{\pm 2\sigma(x + \bar{\gamma}_1)} \quad (53)$$

obtained by multiplying, member by member, equation (51) by the  $\bar{\sigma}^2$  power of equation (50). By identical arguments as above it can be shown that the trajectories that solve (50) and (53) reach the focus at the same “instant”:  $x_0 = -\bar{\gamma}_1$ . Thus, we have shown that the focus is a conjugate point to the vacuum.

We now use the derivatives of (50) and (53) with respect to  $\gamma_2$  to find the Jacobi field orthogonal to each kink trajectory ( $\bar{\mu}_1(x, \bar{\gamma}_1, \gamma_2), \bar{\mu}_2(x, \bar{\gamma}_1, \gamma_2)$ ): if  $\alpha_1 \neq \alpha_2$ ,

$$\frac{-(-1)^{\alpha_1}}{\bar{\mu}_1 \sqrt{1 - \bar{\mu}_1} (\bar{\sigma}^2 - \bar{\mu}_1)} \frac{\partial \bar{\mu}_1}{\partial \gamma_2} - \frac{(-1)^{\alpha_2}}{\bar{\mu}_2 \sqrt{1 - \bar{\mu}_2} (\bar{\sigma}^2 - \bar{\mu}_2)} \frac{\partial \bar{\mu}_2}{\partial \gamma_2} = 2 \quad (54)$$

$$\frac{(-1)^{\alpha_1}}{\bar{\mu}_1 \sqrt{1 - \bar{\mu}_1}} \frac{\partial \bar{\mu}_1}{\partial \gamma_2} + \frac{(-1)^{\alpha_2}}{\bar{\mu}_2 \sqrt{1 - \bar{\mu}_2}} \frac{\partial \bar{\mu}_2}{\partial \gamma_2} = 0 \quad (55)$$

The solution of the linear system of algebraic equations (54-55) is:

$$\frac{\partial \bar{\mu}_1}{\partial \gamma_2} = \frac{2\sqrt{1 - \bar{\mu}_1} \bar{\mu}_1 (\bar{\sigma}^2 - \bar{\mu}_1) (\bar{\sigma}^2 - \bar{\mu}_2)}{(-1)^{\alpha_1} (\bar{\mu}_2 - \bar{\mu}_1)}; \quad \frac{\partial \bar{\mu}_2}{\partial \gamma_2} = \frac{2\sqrt{1 - \bar{\mu}_2} \bar{\mu}_2 (\bar{\sigma}^2 - \bar{\mu}_2) (\bar{\sigma}^2 - \bar{\mu}_1)}{(-1)^{\alpha_2} (\bar{\mu}_2 - \bar{\mu}_1)} \quad (56)$$

The Jacobi field  $V_J^1(x) = \frac{\partial \bar{\mu}_1}{\partial \gamma_2}(x)$ ,  $V_J^2(x) = \frac{\partial \bar{\mu}_2}{\partial \gamma_2}(x)$  is zero at the vacuum point. To check that it is also zero at the focus we take the limit  $\bar{\mu}_1 \rightarrow \bar{\sigma}^2$  from the left, and  $\bar{\mu}_2 \rightarrow \bar{\sigma}^2$  from the right:

$$\lim_{(\bar{\mu}_1, \bar{\mu}_2) \rightarrow (\bar{\sigma}^2, \bar{\sigma}^2)} \frac{\partial \bar{\mu}_1}{\partial \gamma_2} = \lim_{(\bar{\mu}_1, \bar{\mu}_2) \rightarrow (\bar{\sigma}^2, \bar{\sigma}^2)} \frac{4\sigma^2 \bar{\sigma}^2}{(-1)^{\alpha_1}} \frac{1}{\frac{1}{\sqrt{1 - \bar{\mu}_2} - \sigma} - \frac{1}{\sqrt{1 - \bar{\mu}_1} - \sigma}} = 0$$

and the same thing happens to the  $V_J^2$  component. Therefore, the NTK3, NTK2 $\sigma_3$  and NTK2 $\sigma_2$  kinks are not local minima of  $E$ : they are unstable.

## 2. TK3 topological kinks

To identify the Jacobi fields on a given TK3 generic kink, we shall perform an almost identical analysis and shall use equations (44) and (45) to describe the TK3 orbit. We multiply the equation for the TK3 kink form, member by member, by the product of the  $\sigma_3 \bar{\sigma}_2^2$  power of (44) by the  $-\sigma_2 \bar{\sigma}_3^2$  power of (45) to obtain the modified kink form factor equation:

$$\left| \frac{\sqrt{1-\lambda_1}-1}{\sqrt{1-\lambda_1}+1} \right|^{(-1)^{\alpha_1}} \cdot \left| \frac{\sqrt{1-\lambda_2}-1}{\sqrt{1-\lambda_2}+1} \right|^{(-1)^{\alpha_2}} \cdot \left| \frac{\sqrt{1-\lambda_3}-1}{\sqrt{1-\lambda_3}+1} \right|^{(-1)^{\alpha_3}} = e^{2(x+\alpha)} \quad (57)$$

where  $\alpha = \gamma_1 + \frac{\bar{\sigma}_2^4}{\sigma_3^2 - \sigma_2^2} \gamma - \frac{\bar{\sigma}_3^4}{\sigma_2^2 - \sigma_3^2} \bar{\gamma}$ .

The vacuum point is a solution of (57) for  $x = -\infty$ ,  $\alpha_1 = \alpha_2 = \alpha_3 = 0$  and  $x = \infty$ ,  $\alpha_1 = \alpha_2 = \alpha_3 = 1$ . Arguing along the same line as in the NTK case, one finds that any TK3 trajectory hits the hyperbola (64) at the ‘‘instant’’  $x_1 = -\alpha - \frac{1}{2} \ln \left| \frac{\sqrt{1-\tilde{\lambda}_1}-1}{\sqrt{1-\tilde{\lambda}_1}+1} \right|^{(-1)^{\alpha_1}}$  -  $\tilde{\lambda}_1$  is a root of equation (47). The same trajectory reaches the ellipse (63) ‘‘later’’:  $x_2 = -\alpha - \frac{1}{2} \ln \left| \frac{\sqrt{1-\tilde{\lambda}_3}-1}{\sqrt{1-\tilde{\lambda}_3}+1} \right|^{(-1)^{\alpha_3}}$  -  $\tilde{\lambda}_3$  is a root of equation (46). The necessary fine tuning of the ‘‘arrival times’’ to the focal curves depends on the intersection points of the trajectories with these curves. Thus, the focal hyperbola and ellipse are indeed lines of conjugate points to the vacuum.

The implicit derivation of (44), (45) and (57) with respect to  $\gamma$  and  $\bar{\gamma}$ , as well as the solution of the subsequent algebraic linear system, provides the two Jacobi fields orthogonal to each TK3 trajectory:  $\vec{V}_{J_1}(x) = \frac{\partial \vec{\lambda}_{\text{TK3}}}{\partial \gamma}(x)$ ,  $\vec{V}_{J_2}(x) = \frac{\partial \vec{\lambda}_{\text{TK3}}}{\partial \bar{\gamma}}(x)$ . These fields are

$$\begin{aligned} V_{J_1}^1(x) &= -\frac{g^{11}}{\sigma_2^2 - \sigma_3^2} \frac{\partial W}{\partial \lambda_1} (\bar{\lambda}_2 - \bar{\sigma}_3^2)(\bar{\lambda}_3 - \bar{\sigma}_3^2); & V_{J_1}^2(x) &= -\frac{g^{22}}{\sigma_2^2 - \sigma_3^2} \frac{\partial W}{\partial \lambda_2} (\bar{\lambda}_1 - \bar{\sigma}_3^2)(\bar{\lambda}_3 - \bar{\sigma}_3^2) \\ V_{J_1}^3(x) &= \frac{g^{33}}{\sigma_2^2 - \sigma_3^2} \frac{\partial W}{\partial \lambda_3} (\bar{\lambda}_1 - \bar{\sigma}_3^2)(\bar{\lambda}_2 - \bar{\sigma}_3^2) \end{aligned} \quad (58)$$

$$\begin{aligned} V_{J_2}^1(x) &= -\frac{g^{11}}{\sigma_2^2 - \sigma_3^2} \frac{\partial W}{\partial \lambda_1} (\bar{\lambda}_2 - \bar{\sigma}_2^2)(\bar{\lambda}_3 - \bar{\sigma}_2^2); & V_{J_2}^2(x) &= -\frac{g^{22}}{\sigma_2^2 - \sigma_3^2} \frac{\partial W}{\partial \lambda_2} (\bar{\lambda}_1 - \bar{\sigma}_2^2)(\bar{\lambda}_3 - \bar{\sigma}_2^2) \\ V_{J_2}^3(x) &= -\frac{g^{33}}{\sigma_2^2 - \sigma_3^2} \frac{\partial W}{\partial \lambda_3} (\bar{\lambda}_1 - \bar{\sigma}_2^2)(\bar{\lambda}_2 - \bar{\sigma}_2^2) \end{aligned} \quad (59)$$

We have that:

$$\lim_{(\bar{\lambda}_1, \bar{\lambda}_2, \bar{\lambda}_3) \rightarrow (\bar{\lambda}_1, \bar{\sigma}_2^2, \bar{\sigma}_2^2)} V_{J_1}^1 = 0 \quad , \quad \lim_{(\bar{\lambda}_1, \bar{\lambda}_2, \bar{\lambda}_3) \rightarrow (\bar{\lambda}_1, \bar{\sigma}_2^2, \bar{\sigma}_2^2)} V_{J_1}^2 = \frac{0}{0} \quad , \quad \lim_{(\bar{\lambda}_1, \bar{\lambda}_2, \bar{\lambda}_3) \rightarrow (\bar{\lambda}_1, \bar{\sigma}_2^2, \bar{\sigma}_2^2)} V_{J_1}^3 = \frac{0}{0}$$

and the  $V_{J_1}^1$  component of the Jacobi field is zero on the focal hyperbola, whereas  $V_{J_1}^2, V_{J_1}^3$  are indeterminate. To solve for the indeterminacy in the second component, we carefully take the limit of  $V_{J_1}^2$  when  $\bar{\lambda}_2$  and  $\bar{\lambda}_3$  go to  $\bar{\sigma}_2^2$  respectively from the left and from the right:

$$\lim_{(\bar{\lambda}_1, \bar{\lambda}_2, \bar{\lambda}_3) \rightarrow (\bar{\lambda}_1, \bar{\sigma}_2^2, \bar{\sigma}_2^2)} V_{J_1}^2 = \frac{4\sigma_2^2 \bar{\sigma}_2^2 (\tilde{\lambda}_1 - \bar{\sigma}_3^2)}{(\tilde{\lambda}_1 - \bar{\sigma}_2^2)(-1)^{\alpha_1}} \lim_{(\bar{\lambda}_1, \bar{\lambda}_2, \bar{\lambda}_3) \rightarrow (\bar{\lambda}_1, \bar{\sigma}_2^2, \bar{\sigma}_2^2)} \frac{1}{\frac{1}{\sqrt{1-\bar{\lambda}_2-\sigma_2}} - \frac{1}{\sqrt{1-\bar{\lambda}_3-\sigma_2}}} = 0$$

The same limit shows that the third component is also zero on the focal hyperbola and that the Jacobi field  $\vec{V}_{J_1}(x)$  is zero at the intersection points of the TK3 trajectory with the hyperbola (47). The zeroes of the other Jacobi field,  $\vec{V}_{J_2}(x)$ , are the vacuum point and the intersection point of the kink trajectory with the ellipse (46). The TK3 kinks are saddle points of the energy functional and therefore are unstable.

## 4.2 The spectrum of the Hessian for the non-generic topological kinks

Non-generic topological kinks are very singular points at the boundary of the kink moduli space and the extension of this procedure to them could cast doubt on its applicability. Fortunately, analytical formulas both for the kink orbit and form factors are available in Cartesian coordinates and one can directly look at the spectrum of the Hessian:

$$\Delta \vec{V} = \sum_{a=1}^3 \sum_{b=1}^3 \Delta_b^a V^b \vec{e}_a \quad .$$

### 4.2.1 TK1 Hessian

In this case the Hessian is a diagonal matrix,  $\Delta_b^a = 0, a \neq b$ , of Schrodinger operators

$$\Delta_1^1 = -\frac{d^2}{dx^2} + 4 - \frac{6}{\cosh^2 x} \quad , \quad \Delta_2^2 = -\frac{d^2}{dx^2} + \sigma_2^2 - \frac{2}{\cosh^2 x} \quad , \quad \Delta_3^3 = -\frac{d^2}{dx^2} + \sigma_3^2 - \frac{2}{\cosh^2 x} \quad (60)$$

with potential wells of Pösch-Teller type. The spectrum is shown in the next Table:

$\Delta_1^1$	$\Delta_2^2$	$\Delta_3^3$
$(0) \sqcup (3) \sqcup (k_1^2 + 4)$	$(-\sigma_2^2) \sqcup (0) \sqcup (k_2^2 + \sigma_2^2)$	$(-\sigma_3^2) \sqcup (0) \sqcup (k_3^2 + \sigma_3^2)$
$\vec{V}_{(0)}(x) = \text{sech}^2 x \vec{e}_1$	$\vec{V}_{(-\sigma_2^2)}(x) = \text{sech} x \vec{e}_2$	$\vec{V}_{(-\sigma_3^2)}(x) = \text{sech} x \vec{e}_3$
$\vec{V}_{(3)}(x) = \frac{\tanh x}{\cosh x} \vec{e}_1$	$\vec{V}_{J_2}(x) = e^{\sigma_2 x} (\sigma_2 - \tanh x) \vec{e}_2$	$\vec{V}_{J_3}(x) = e^{\sigma_3 x} (\sigma_3 - \tanh x) \vec{e}_3$
$\vec{V}_{(k_1^2)}(x) = e^{ik_1 x} P_2(\tanh x) \vec{e}_1$	$\vec{V}_{(k_2^2)}(x) = e^{ik_2 x} P_1(\tanh x) \vec{e}_2$	$\vec{V}_{(k_3^2)}(x) = e^{ik_3 x} P_1(\tanh x) \vec{e}_3$

Here,  $k_1, k_2, k_3 \in \mathbb{R}$  and  $P_l(\tanh x)$  is the  $l^{\text{th}}$  Jacobi polynomial. The spectrum of  $\Delta$  contains two negative eigenvalues obeying small fluctuations in the directions orthogonal to the kink orbit. The TK1 kink is a saddle point of  $E[\vec{\phi}]$  and is therefore unstable. The Jacobi fields  $\vec{V}_{J_1}$  and  $\vec{V}_{J_2}$  are both zero at  $x = -\infty$  when the trajectory departs from the vacuum point  $\vec{v} = -\vec{e}_1$ , and reach a second zero respectively at  $x = \text{arctanh} \sigma_2$ ,  $x = \text{arctanh} \sigma_3$ , the points where the foci  $F_2 \equiv (\sigma_2, 0, 0)$ ,  $F_3 \equiv (\sigma_3, 0, 0)$  are hit by the TK1 trajectory, as expected.

### 4.2.2 TK2 $\sigma_3$ and TK2 $\sigma_2$ Hessians

The Hessian for the TK2 $\sigma^3$  kink is non-diagonal:

$$\Delta \vec{V} \equiv \begin{pmatrix} -\frac{d^2}{dx^2} + 4 - \frac{2(2+\sigma_3^2)}{\cosh^2(\sigma_3 x)} & 0 & 4\bar{\sigma}_3 \frac{\tanh(\sigma_3 x)}{\cosh(\sigma_3 x)} \\ 0 & -\frac{d^2}{dx^2} + \sigma_2^2 - \frac{2\sigma_3^2}{\cosh^2(\sigma_3 x)} & 0 \\ 4\bar{\sigma}_3 \frac{\tanh(\sigma_3 x)}{\cosh(\sigma_3 x)} & 0 & -\frac{d^2}{dx^2} + \sigma_3^2 - \frac{2(3\sigma_3^2-2)}{\cosh^2(\sigma_3 x)} \end{pmatrix} \begin{pmatrix} V^1 \\ V^2 \\ V^3 \end{pmatrix}$$

We simply study the spectrum of  $\Delta_2^2$ , governing the small fluctuations in the direction orthogonal to the  $\vec{e}_1; \vec{e}_3$  plane, where the TK2 $\sigma_3$  kink lives. The first eigenvalue,  $\sigma_2^2 - \sigma_3^2$ , with an eigen-function  $\vec{V}_{(\sigma_2^2 - \sigma_3^2)}(x) = \frac{1}{\cosh(\sigma_3 x)} \vec{e}_2$ , shows that the TK2 $\sigma_3$  kink is a saddle point of  $E[\vec{\phi}]$ ; it is, therefore, unstable. Moreover, there is a Jacobi field  $\vec{V}_J(x) = e^{\sigma_2 x} \left( \frac{\sigma_2}{\sigma_3} - \tanh(\sigma_3 x) \right) \vec{e}_2$ , which, besides the vacuum point, is zero at the umbilicus:  $x = \frac{1}{\sigma_3} \operatorname{arctanh} \frac{\sigma_2}{\sigma_3}$  yields  $\phi^1 = \frac{\sigma_2}{\sigma_3}$ , which is the umbilicus point of the ellipsoid on the TK2 $\sigma_3$  orbit. After crossing the umbilicus, this field can be glued in a continuous but not differentiable way to the  $\vec{V}_{J_2}$  Jacobi field on the TK1 kink beyond the focus  $F_2$ . The new field can be understood as a Jacobi field associated with the  $T_2^{\sigma_2} T_2^{\sigma_3} T_1$  limit of the TK3 moduli space. Note that there are also eigen-functions in the continuous spectrum with eigenvalues  $k^2 \sigma_3^2 + \sigma_2^2$ .

The Hessian for the TK2 $\sigma_2$  kink is almost identical:

$$\Delta \vec{V} \equiv \begin{pmatrix} -\frac{d^2}{dx^2} + 4 - \frac{2(2+\sigma_2^2)}{\cosh^2(\sigma_2 x)} & 4\bar{\sigma}_2 \frac{\tanh(\sigma_2 x)}{\cosh(\sigma_2 x)} & 0 \\ 4\bar{\sigma}_2 \frac{\tanh(\sigma_2 x)}{\cosh(\sigma_2 x)} & -\frac{d^2}{dx^2} + \sigma_2^2 - \frac{2(3\sigma_2^2 - 2)}{\cosh^2(\sigma_2 x)} & 0 \\ 0 & 0 & -\frac{d^2}{dx^2} + \sigma_3^2 - \frac{2\sigma_2^2}{\cosh^2(\sigma_2 x)} \end{pmatrix} \begin{pmatrix} V^1 \\ V^2 \\ V^3 \end{pmatrix}$$

The non-diagonal box, however, governs small fluctuations on the  $\vec{e}_1; \vec{e}_2$  plane, instead of on the  $\vec{e}_1; \vec{e}_3$  plane. The most important difference is that the Jacobi field  $\vec{V}_J(x) = e^{\sigma_3 x} \left( \frac{\sigma_3}{\sigma_2} - \tanh(\sigma_2 x) \right) \vec{e}_3$  of  $\Delta_3^3$  is only zero at the vacuum point on the TK2 $\sigma_2$  trajectory. This field intersects the Jacobi field  $\vec{V}_{J_3}$  on the TK1 kink -after this latter has crossed the focus  $F_3$ - and both form a new Jacobi field on the  $T_2^{\sigma_2} T_2^{\sigma_3} T_1$  kink configuration. The spectrum of  $\Delta_3^3$  starts with the positive eigenvalue  $\sigma_3^2 - \sigma_2^2$  and the TK2 $\sigma_2$  kink is stable against small fluctuations that bring the orbit away from the  $\vec{e}_1; \vec{e}_2$  plane.

Concerning fluctuations of the form  $\vec{V}(x) = V^1(x)\vec{e}_1 + V^2(x)\vec{e}_2$ , we cannot explicitly compute the spectrum of  $\Delta$ : one should find the stationary states for a quantum  $\frac{1}{2}$  spin particle moving through a non-constant spin-exchange potential. Nevertheless, because TK2 $\sigma_2$  is an absolute minimum of the energy, there cannot be negative eigenvalues in  $\operatorname{Spec} \Delta$ . In fact, we know the translational mode:  $\vec{V}_{(0)}(x) = \frac{1}{\cosh(\sigma_2 x)} (\vec{e}_1 - \bar{\sigma}_2 \sinh(\sigma_2 x) \vec{e}_2)$ , which is tangent to the TK2 $\sigma_2$  orbit. There must also be a Jacobi field, null only at the vacuum point, along the TK2 $\sigma_2$  orbit. This Jacobi field is completed by  $\vec{V}_{J_2}(x)$  after their intersection, which occurs before the crossing of  $\vec{V}_{J_2}(x)$  by  $F_2$ .

### 4.3 Morse theory of kinks

Let  $\Omega M^n = \{\gamma : S^1 \rightarrow M^n / \gamma(0) = \gamma(1) = m_0\}$  be the space of closed paths with a fixed base point  $m_0$  in a Riemannian manifold  $M^n$ . Morse theory establishes a link between the topology of  $\Omega M^n$  and the ‘‘critical point’’ structure of a well-defined functional in  $\Omega M^n$ , [12]. A formulation of this theory à la Bott, [13], is as follows:

Let  $P_t(\Omega M^n) = \sum_{k=0}^{\infty} b_k t^k$  be the Poincarè series of  $\Omega M^n$  in the indeterminate  $t$ . The topology of  $\Omega M^n$  is encoded in  $P_t(\Omega M^n)$  because  $b_k = \dim H_k(\Omega M^n, \mathbb{R})$  are the Betti numbers that account for the dimension of the  $k^{\text{th}}$  homology group of  $\Omega M^n$ . Let  $\mathcal{M}_t(E) = \sum_{N_c} P_t(N_c) t^{\mu(N_c)}$  be the Morse series of the  $E$  functional.  $\mathcal{M}_t(E)$  encodes the critical point structure of  $E$ : the sum is over the critical manifolds  $N_c$  formed either by a single isolated



critical path or by continuous sets of critical paths, depending on  $M^n$ .  $P_t(N_c)$  is the Poincaré polynomial of  $N_c$  and the most important ingredient is the Morse index  $\mu(N_c)$ :

$\mu(N_c)$  is the dimension of the sub-space in the tangent space  $T_{\gamma_c}\Omega M^n$  where the Hessian quadratic form of  $L$  at  $\gamma_c \in N_c$  is negative definite in the directions orthogonal to  $N_c$ . The Morse inequalities,

$$\mathcal{M}_t(E) \geq P_t(\Omega M^n)$$

tell us that the topology of  $\Omega M^n$  forces the existence of most of the critical points of  $E$ .

The Morse index can also be understood as the number of negative eigenvalues of the Hessian operator and hence  $\mu(N_c)$  informs us about the (lack of) stability of a given critical path  $\gamma_c$ . On the other hand, one can skip the solving of a difficult spectral problem to compute  $\mu(N_c)$  by applying the Morse index theorem:

“The Morse index of a critical path  $\gamma_c$  is equal to the number of conjugate points to the base point crossed by  $\gamma_c$  counted with multiplicity”. Recall that conjugate points to  $m_0$  are those points in  $M^n$  where infinite critical paths passing through  $m_0$  meet again and the multiplicity is the dimension of a section transverse to this congruence near the focal point, [8] and [9].

In this sub-Section we shall develop the Morse theory of kinks in our system as a synthetic approach for dealing with the stability problem. We have the following dictionary:  $M^n$  is the manifold  $\bar{\mathbf{P}}_3(0)$ ;  $\Omega M^n$  is the full configuration space  $\mathcal{C}$ . Note that in elliptic coordinates the four disconnected sectors are melded in a single sector:  $\mathcal{C} = \mathcal{C}^{11} \sqcup \mathcal{C}^{12} \sqcup \mathcal{C}^{21} \sqcup \mathcal{C}^{22}$ . A topology in  $\mathcal{C}$  is defined in Reference [9]. The real homology of  $\mathcal{C}$  is also analysed in [9].  $m_0$  is the vacuum point  $D$  in  $\bar{\mathbf{P}}_3(0)$ .

The conjugate points to D have been determined in the previous sub-sections §4.1 and §4.2 as zero loci of the Jacobi fields. We summarize the results as follows:

- (1). If  $\lambda_1 = \bar{\sigma}_3^2 = \lambda_2$ . Every point in the  $F_1F_3$  edge is a conjugate point to D. Through any point in the focal line,  $F_1F_3$  crosses a one-parameter congruence of kink trajectories, the multiplicity of the conjugate points in  $F_1F_3$  is 1.
- (2). If  $\lambda_2 = \bar{\sigma}_2^2 = \lambda_3$ . Each point in the  $AF_2$  edge is also a conjugate point to D.  $AF_2$  is a focal line formed by conjugate points of multiplicity 1.

The points A,  $F_2$  and  $F_3$  are also conjugate points. In fact, these points are crossed by the kinks belonging to two one-dimensional families. The trajectories in the kink moduli spaces  $\mathcal{M}_{N_3T_1}$  and  $\mathcal{M}_{N_2^{\sigma_3}T_2^{\sigma_2}}$  pass through the  $F_3$  focus; either the  $N_3T_1$  or the  $N_2^{\sigma_3}T_2^{\sigma_2}$  family is reached, depending on which path in  $\mathcal{M}_{T_3}$  is chosen. Simili modo, all the kink trajectories in both  $\mathcal{M}_{N_3T_1}$  and  $\mathcal{M}_{N_2^{\sigma_2}T_2^{\sigma_3}}$  coincide at the umbilicus A and the  $F_2$  focus; again, the two possibilities arise in connection with the existence of two paths in  $\mathcal{M}_{T_3}$  that lead to different families of singular kinks.

Finally D itself can be viewed as a conjugate point of multiplicity 2; there is a two-parameter congruence of kink trajectories emanating from D.

### 4.3.1 The Morse series of $\mathcal{C}$

We now apply the Morse index theorem to compute the Morse index of the kink trajectories.

**I.** Vacuum trajectory: D. Morse index,  $\mu(D) = 0$ . Here, we include the computation of the  $\text{TK}2\sigma_2$  kink as the only stable configuration, and therefore consider the edge DC deformed continuously to the vacuum point D.

**II.**  $\text{TK}2\sigma_3 \sqcup \text{AK}2\sigma_3$ .

The  $\text{TK}2\sigma_3$  trajectory starts from D, passes through the umbilicus point A, reaches the point B, and comes back to D along the same path. A subtle point is that only in the second crossing is the A point a conjugate point to D along the  $\text{TK}2\sigma_3$  trajectory because the last crossing happens at the same time as a congruence of  $\text{N}_3\text{T}_1$  kinks reaches point A in the edge  $\text{AF}_2$  in its first crossing. Another even more subtle point is the following: we are considering closed trajectories, but the  $\text{TK}2\sigma_3$  trajectory is closed only in  $\bar{\mathbf{P}}_3(0)$ . If we require trajectories also closed in Euclidean space, the  $\text{TK}2\sigma_3$  trajectory must be counted together with the anti-kink  $\text{AK}2\sigma_3$ . Again, only in the second crossing along the  $\text{AK}2\sigma_3$  trajectory is the umbilicus point A a conjugate point to D. Therefore, the Morse index of the  $\text{TK}2\sigma_3 \sqcup \text{AK}2\sigma_3$  trajectory is two:  $\mu(\text{TK}2\sigma_3 \sqcup \text{AK}2\sigma_3) = 2$ . Note that the second crossing of the  $\text{TK}3$  and  $\text{AK}3$  trajectories though A are simultaneous and that D is only the starting and ending point of this super-imposed kink.

**III.**  $\text{TK}1 \sqcup \text{AK}1$ .

Both the  $\text{TK}1$  and  $\text{AK}1$  trajectories pass through the conjugate points to D  $\text{F}_2$  and  $\text{F}_3$  twice, but only in the second crossing are they truly conjugate points to D because then, these points are reached by the  $\text{TK}3$  or  $\text{AK}3$  congruences for the first time. Therefore, the Morse index of the  $\text{TK}1 \sqcup \text{AK}1$  trajectory is four:  $\mu(\text{TK}1 \sqcup \text{AK}1) = 4$ .

**IV.**  $\text{TK}3 \sqcup \text{AK}3$ .

A  $\text{TK}3$  trajectory hits the  $\text{F}_1\text{F}_3$  edge once and the  $\text{AF}_2$  edge twice, whereas the anti-kink  $\text{AK}3$  trajectory does the same in the opposite sense. Therefore,  $\mu(\text{TK}3 \sqcup \text{AK}3) = 6$ . The critical manifold formed by these configurations is:  $\mathcal{N}_c = \bar{\mathcal{M}}_{T_3}^{(3)} \sqcup \bar{\mathcal{M}}_{A_3}^{(3)}$ . We have chosen the compactification of  $\mathcal{M}_{T_3}$  described in sub-Section §3.3: it is understood that in the count of a trajectory passing through A,  $\text{F}_2$  or  $\text{F}_3$  the appropriate  $\text{N}_3\text{T}_1$ ,  $\text{N}_2^{\sigma_3}\text{T}_2^{\sigma_2}$  or  $\text{N}_2^{\sigma_3}\text{T}_2^{\sigma_2}$  congruence is taken into account. In any case,  $P_t(\bar{\mathcal{M}}_{T_3}^{(3)} \sqcup \bar{\mathcal{M}}_{A_3}^{(3)}) = 1 + t^2$  and the contribution to the Morse series is  $(1 + t^2)t^6$ .

In fact, these are the only kink trajectories that should be included, because all of them starts and end at D. Strictly speaking, D cannot be crossed by any trajectory because D only can be reached again in infinite “time”.

Closing our eyes to this fact, the next critical manifold is:

**V.**  $(\text{TK}2\sigma_3 \# \text{TK}3(1)) \sqcup (\text{AK}2\sigma_3 \# \text{AK}3(1))$ .

The  $\text{TK}2\sigma_3$  trajectory is followed by a single  $\text{TK}3(1)$  kink: precisely  $\text{T}_2^{\sigma_2}\text{T}_2^{\sigma_3}\text{T}_1$ . The two trajectories are glued (represented by the symbol  $\#$ ) at point D. The crossing of D, which is shared by the composite kink and the anti-kink trajectories, contributes to the Morse index with 2 because of the multiplicity:

$$\mu((\text{T}_2^{\sigma_3} \# \text{T}_2^{\sigma_2}\text{T}_2^{\sigma_3}\text{T}_1) \sqcup (\text{A}_2^{\sigma_3} \# \text{A}_2^{\sigma_2}\text{A}_2^{\sigma_3}\text{A}_1)) = 10$$

**VI.**  $(\text{TK}1 \# \text{TK}3(1)) \sqcup (\text{AK}1 \# \text{AK}3(1))$ .

For the same reasons,

$$\mu((\text{T}_1 \# \text{T}_2^{\sigma_2}\text{T}_2^{\sigma_3}\text{T}_1) \sqcup (\text{A}_1 \# \text{A}_2^{\sigma_2}\text{A}_2^{\sigma_3}\text{A}_1)) = 12$$

## VII. (TK3 # TK3) $\sqcup$ (AK3 # AK3).

The gluing of two families of TK3 and AK3 kinks again requires the application of degenerate Morse theory. The Morse index of one member of the family is  $\mu((\text{TK3}\#\text{TK3}) \sqcup (\text{AK3}\#\text{AK3})) = 14$  but the Poincarè polynomial of this critical manifold is:  $P_t((\bar{\mathcal{M}}_{T_3}\#\bar{\mathcal{M}}_{T_3}) \sqcup (\bar{\mathcal{M}}_{A_3}\#\bar{\mathcal{M}}_{A_3})) = 1 + t^2$ .

Iteration of these basic elements produces the Morse series:

$$\begin{aligned} \mathcal{M}_t(E|_{\mathcal{C}}) &= 1 + (1+t^2)t^2 + (1+t^2)t^6 + (1+t^2)t^{10} + (1+t^2)t^{14} + \dots \\ &= 1 + (1+t^2) \sum_{k=0}^{\infty} t^{2(2k+1)} = \frac{1}{1-t^2} \end{aligned}$$

Because all the coefficients of the odd powers of  $t$  in  $\mathcal{M}_t$  are zero, the lacunary principle states that the Morse inequality becomes equality, [13]:

$$\mathcal{M}_t(E|_{\mathcal{C}}) = P_t(\mathcal{C}) = \frac{1}{1-t^2} = P_t(\Omega S^3)$$

The configuration space is of the same homology type as  $\Omega S^3$ : the loop space in  $S^3$ . There is some kind of topological universality and the first terms in  $\mathcal{M}_t(E|_{\mathcal{C}})$  tell us that the existence of  $\text{TK}2\sigma_3 \sqcup \text{AK}2\sigma_3$  kinks is due to the fact that the homology group  $H_2(\mathcal{C}, \mathbb{R}) = \mathbb{R}$  is non-trivial; the  $\text{TK}1 \sqcup \text{AK}1$  kink comes from  $H_4(\mathcal{C}, \mathbb{R}) = \mathbb{R}$ ; the  $\text{TK}3 \sqcup \text{AK}3$  family corresponds to  $H_6(\mathcal{C}, \mathbb{R}) = \mathbb{R}$ , and so forth.

### 4.3.2 Kink stability from the index theorem

We have shown in sub-sections §4.1 and §4.2 that in the topological sectors  $\mathcal{C}^{12}$  and  $\mathcal{C}^{21}$  only the  $\text{TK}2\sigma_2$  and  $\text{AK}2\sigma_2$  kinks are stable, whereas in the non-topological sectors  $\mathcal{C}^{11}$  and  $\mathcal{C}^{22}$  only the ground states  $v^1$  and  $v^2$  are stable. The degree of instability of each kind of kink is measured by the Morse index, which agrees with the number of kink configurations with lower energy in the same topological sector. We have a situation of stratified Morse theory according to the energy hierarchy in each topological sector:

A.  $\mathcal{C}^{12}$  and  $\mathcal{C}^{21}$ :

$$\begin{aligned} E(\text{TK}3) &> E(\text{TK}1) > E(\text{TK}2\sigma_3) > E(\text{TK}2\sigma_2) \\ E(\text{AK}3) &> E(\text{AK}1) > E(\text{AK}2\sigma_3) > E(\text{AK}2\sigma_2) \end{aligned}$$

B.  $\mathcal{C}^{11}$  and  $\mathcal{C}^{22}$ :  $\alpha = 1, 2$

$$E(\text{NTK}2\sigma_3(\alpha)) > E(\text{NTK}2\sigma_2(\alpha)) > E(\text{NTK}3(\alpha)) > E(v^\alpha)$$

where  $\text{NTK}(\alpha)$  means that the NTK family starts from the vacuum  $v^\alpha$ .

To check this statement, we simply apply the Morse index theorem to compute the Morse index of each kink in the system .

1. Kinks in the topological sector  $\mathcal{C}^{12}$ :

- A.  $\mu(\text{TK3}) = 3$ . The application of the Morse index theorem to a TK3 trajectory works as follows: the trajectory starts at the ground state  $v^1$ , goes to the focal hyperbola  $\frac{\phi_1^2}{\sigma_2^2} - \frac{\phi_3^2}{\sigma_3^2 - \sigma_2^2} = 1$ , comes back to the focal ellipse  $\frac{\phi_1^2}{\sigma_3^2} + \frac{\phi_2^2}{\sigma_3^2 - \sigma_2^2} = 1$ , reaches the focal hyperbola (the other branch) again, and ends at  $v^2$ . Therefore, a TK3 trajectory crosses three c. p. to D, each of multiplicity one. There are three orthogonal directions of instability in  $\mathcal{C}$  for any TK3 kink.
- B.  $\mu(\text{TK1}) = 2$ . It is easy to repeat in Cartesian coordinates the arguments presented in elliptic coordinates above, in order to conclude that the Morse index of a TK1 kink is 2. The TK1 trajectory crosses the foci  $F_2$  and  $F_3$  of the ellipsoid  $\phi_1^2 + \frac{\phi_2^2}{\sigma_2^2} + \frac{\phi_3^2}{\sigma_3^2} = 1$  twice, but only in the second crossing are the foci reached by the NTK2 $\sigma_2$  or NTK2 $\sigma_3$  trajectories. There are only two directions of instability near the TK1 kink, as has been explicitly shown in sub-section §4.2.2.
- C.  $\mu(\text{TK2}\sigma_3) = 1$ . A TK2 $\sigma_3$  trajectory crosses two umbilicus points in the ellipsoid, but only in the second crossing is the umbilicus point a conjugate point to  $v^1$  along the TK2 $\sigma_3$  path because all the NTK3 congruence reaches the second umbilicus at the same instant as TK2 $\sigma_3$ . The direction of instability in  $\mathcal{C}$  near TK2 $\sigma_3$  has also been shown in sub-section §4.2.2.
- D.  $\mu(\text{TK2}\sigma_2) = 0$ . The TK2 $\sigma_2$  trajectories do not cross any focal lines and their Morse index is zero. Again, in sub-section §4.2.2 we saw that there are no directions of instability near TK2 $\sigma_2$  by showing that the Hessian quadratic form of  $E$  at TK2 $\sigma_2$  is semi-definite positive.

## 2. Kinks in the non-topological sector $\mathcal{C}^{11}$ :

- A.  $\mu(\text{NTK2}\sigma_3) = 3$ . Any NTK2 $\sigma_3$  trajectory hits the focal hyperbola  $\frac{\phi_1^2}{\sigma_2^2} - \frac{\phi_3^2}{\sigma_3^2 - \sigma_2^2} = 1$  four times. Only during the second and fourth crossings does the NTK2 $\sigma_3$  trajectory reach conjugate points to  $v^1$ .

The time table is as follows: 1) the second crossing of the NTK2 $\sigma_3$  trajectory by the focal hyperbola coincides with the first crossing of a TK3 congruence. 2) The NTK2 $\sigma_3$  kink crosses the  $F_3$  focus at the same time as any other NTK2 $\sigma_3$ . 3) The fourth crossing of the NTK2 $\sigma_3$  trajectory by the focal hyperbola (second branch) happens simultaneously to the crossing of the TK3 congruence. Therefore, the Morse index of the NTK2 $\sigma_3$  is 3: there are three directions of instability in  $T_{\text{NTK2}\sigma_3}\mathcal{C}$ .

- B.  $\mu(\text{NTK2}\sigma_2) = 2$ . Any NTK2 $\sigma_2$  trajectory hits the focal ellipse  $\frac{\phi_1^2}{\sigma_3^2} + \frac{\phi_2^2}{\sigma_3^2 - \sigma_2^2} = 1$  twice. Only during the second crossing does the NTK2 $\sigma_2$  trajectory reach a conjugate point to  $v^1$ . The time table is as follows: 1) All the members of the NTK2 $\sigma_2$  congruence meet at the  $F_2$  focus at the same time.  $F_2$  is thus a conjugate point to  $v^1$  with multiplicity one. 2) The second crossing of the NTK2 $\sigma_2$  kinks through the focal ellipse is simultaneous to the crossing of a TK3 congruence; it is the second conjugate point of multiplicity one to  $v^1$  along any NTK2 $\sigma_2$  kink. The first crossing of the focal ellipse, however, does not correspond to a conjugate point to  $v^2$ . The Morse index is 2: there are two orthogonal instability directions in  $T_{\text{NTK2}\sigma_2}\mathcal{C}$ .

C.  $\mu(\text{NTK3}) = 1$ . Any member of the NTK3 family intersects at an umbilicus point at the same time. The umbilicus is the only conjugate point, with multiplicity one, to  $v^1$  along the NTK3 trajectory and the NTK3 Morse index is one.

D.  $\mu(v^1) = 0$ . The only stable trajectory in  $\mathcal{C}^{11}$  is the ground state  $v^1$ .

In sum, there is a stratification of each connected component  $\mathcal{C}^{\alpha\beta}$  of the configuration space  $\mathcal{C}$  by the ‘‘critical’’ points of the functional  $E$ . Morse’s theory relates the structure of such critical points with the homology of the configuration space itself.

## 5 Further Comments

The stability characteristics of classical solutions in field theory provide qualitative insight about the behaviour of the quantum kink descendants in the semi-classical limit that usually survives strong quantum fluctuations. Therefore, there is a bona fide quantum  $\text{TK}2\sigma_2$  kink state which belongs to the spectrum of the quantum Hamiltonian of the system. The energy up to one-loop order is:

$$\hat{E}[\vec{\Phi}_{T_2^{\sigma_2}}] = E[\vec{\Phi}_{T_2^{\sigma_2}}] + \frac{\hbar}{2}c_d \left( \text{Tr}K^{\frac{1}{2}}(\vec{\Phi}_{T_2^{\sigma_2}}) - \text{Tr}K^{\frac{1}{2}}(\vec{\Phi}_V) + \Delta_m(\vec{\Phi}_{T_2^{\sigma_2}}) - \Delta_m(\vec{\Phi}_V) \right) + O(\hbar^2)$$

Here,

$$K_{ab}(\vec{\Phi}_C) = -\frac{d^2}{dx^2} + \frac{\delta^2 U}{\delta\phi^a\delta\phi^b}|_{\vec{\Phi}_C},$$

$c_d$  is a dimension-full parameter, and

$$\Delta_m(\vec{\Phi}_C) = \sum_{a=1}^3 \delta m_{aa} \cdot \int dx \frac{\delta^2 U}{\delta\phi^a\delta\phi^a}|_{\vec{\Phi}_C}$$

are the counter-terms induced by mass renormalization to take care of the infinite  $\delta m_{aa}$  contributions coming from the tadpole graphs.

All the other kink solutions give rise to resonant states because they are ‘‘sphalerons’’ rather than solitons and decay either to the vacuum or the  $\text{TK}2\sigma_2$  kink, as explained in Reference [16].

## Appendix: The super-potential in Cartesian coordinates

Solving for  $\lambda_1, \lambda_2, \lambda_3$  in (7) as functions of  $\phi_1, \phi_2, \phi_3$  demands that one must solve:

$$\sum_{a=1}^3 \frac{\phi_a^2}{\bar{\sigma}_a^2 - \lambda} = 1, \quad (61)$$

(see Appendix in Reference [1]) which can be written as a cubic algebraic equation in the complex variable  $\lambda \in \mathbb{C}$ . Cardano’s formulae provides the roots of the cubic in the form:

$$\begin{aligned} \lambda_1 &= -\sqrt{|q|} \left( \cos \frac{\theta}{3} + \sqrt{3} \sin \frac{\theta}{3} \right) - \frac{u - A_1}{3}; & \lambda_2 &= -\sqrt{|q|} \left( \cos \frac{\theta}{3} - \sqrt{3} \sin \frac{\theta}{3} \right) - \frac{u - A_1}{3} \\ \lambda_3 &= 2\sqrt{|q|} \cos \frac{\theta}{3} - \frac{u - A_1}{3} \end{aligned}$$

where

$$\begin{aligned}
|q| = -q &= \frac{1}{9} \left( (\phi_1^2 + \phi_2^2 + \phi_3^2)^2 - (\sigma_2^2 + \sigma_3^2) \phi_1^2 + (2\sigma_2^2 - \sigma_3^2) \phi_2^2 + (2\sigma_3^2 - \sigma_2^2) \phi_3^2 + \sigma_2^4 + \sigma_3^4 - \sigma_2^2 \sigma_3^2 \right) \\
r &= \frac{-1}{54} (2(\sigma_2^6 + \sigma_3^6) - 3(\sigma_2^4 \sigma_3^2 + \sigma_2^2 \sigma_3^4)) + \frac{1}{18} (\sigma_2^4 + \sigma_3^4 - 4\sigma_2^2 \sigma_3^2) \cdot (\phi_1^2 + \phi_2^2 + \phi_3^2) + \\
&\quad + \frac{1}{18} (\sigma_2^2 + \sigma_3^2) (\phi_1^2 + \phi_2^2 + \phi_3^2)^2 - \frac{1}{6} (\phi_1^2 + \phi_2^2 + \phi_3^2) (\sigma_2^2 \phi_2^2 + \sigma_3^2 \phi_3^2) + \\
&\quad + \frac{1}{6} (2\sigma_2^2 \sigma_3^2 - \sigma_2^4) \phi_2^2 + \frac{1}{6} (2\sigma_2^2 \sigma_3^2 - \sigma_3^4) \phi_3^2 - \frac{1}{27} (\phi_1^2 + \phi_2^2 + \phi_3^2)^3
\end{aligned}$$

and the angle  $\theta = \arctan \frac{\sqrt{|q^3+r^2|}}{r}$  is defined in the open interval:  $\theta \in (0, \pi)$ . Note that: (a)  $q^3 + r^2$  is semi-definite negative;  $q^3 + r^2 \neq 0$  implies three distinct real roots. (b)  $\theta = 0$  and  $\theta = \pi$  correspond to  $|q^3 + r^2| = 0$  and hence these are values where the square root is ill-defined. (c) choosing another open interval,  $\theta \in (\pi, 2\pi)$  for instance, leads to a permutation of the  $\lambda_a$  roots due to the  $\mathbb{Z}_3$  symmetry.

Using the previous results we write the super-potential in Cartesian coordinates:

$$\begin{aligned}
W^{(\alpha_1, \alpha_2, \alpha_3)}(\phi_1, \phi_2, \phi_3) &= \frac{1}{3\sqrt{3}} \left[ (-1)^{\alpha_1} \sqrt{\sigma_2^2 + \sigma_3^2 + (\phi_1^2 + \phi_2^2 + \phi_3^2) - 6\sqrt{|q|} \cos \frac{\theta}{3}} \right. \\
&\quad \cdot \left( 9 - \sigma_2^2 - \sigma_3^2 - (\phi_1^2 + \phi_2^2 + \phi_3^2) + 6\sqrt{|q|} \cos \frac{\theta}{3} \right) \\
+ &(-1)^{\alpha_2} \sqrt{\sigma_2^2 + \sigma_3^2 + (\phi_1^2 + \phi_2^2 + \phi_3^2) + 3\sqrt{|q|} \left( \cos \frac{\theta}{3} - \sqrt{3} \sin \frac{\theta}{3} \right)} \cdot \\
&\quad \cdot \left( 9 - \sigma_2^2 - \sigma_3^2 - (\phi_1^2 + \phi_2^2 + \phi_3^2) + 3\sqrt{|q|} \left( -\cos \frac{\theta}{3} + \sqrt{3} \sin \frac{\theta}{3} \right) \right) \\
+ &(-1)^{\alpha_3} \sqrt{\sigma_2^2 + \sigma_3^2 + (\phi_1^2 + \phi_2^2 + \phi_3^2) + 3\sqrt{|q|} \left( \cos \frac{\theta}{3} + \sqrt{3} \sin \frac{\theta}{3} \right)} \cdot \\
&\quad \cdot \left. \left( 9 - \sigma_2^2 - \sigma_3^2 - (\phi_1^2 + \phi_2^2 + \phi_3^2) - 3\sqrt{|q|} \left( \cos \frac{\theta}{3} + \sqrt{3} \sin \frac{\theta}{3} \right) \right) \right] \tag{62}
\end{aligned}$$

It is not difficult to identify the singular loci of  $W^{(\alpha_1, \alpha_2, \alpha_3)}$ , and hence of the first-order equations (4), where the super-potential is not continuously differentiable. As one can easily guess, this happens when  $|q^3 + r^2| = 0$  and there are two possibilities: (a) if  $|q^3 + r^2| = 0$  and  $r = \text{constant} > 0$ , i.e.  $\theta = 0$ , the points of non-differentiability of  $W^{(\alpha_1, \alpha_2, \alpha_3)}$  occur at the edge  $\lambda_1 = \lambda_2 = \bar{\sigma}_3^2$  of  $\mathbf{P}_3(\infty)$  or, in the ellipse :

$$\frac{\phi_1^2}{\sigma_3^2} + \frac{\phi_2^2}{\sigma_3^2 - \sigma_2^2} = 1 \tag{63}$$

in  $\mathbb{R}^3$ . (b) if, besides  $|q^3 + r^2| = 0$ ,  $r = \text{constant} < 0$ , i.e.  $\theta = \pi$ , the singular curve is  $\lambda_2 = \lambda_3 = \bar{\sigma}_2^2$ , or the hyperbola

$$\frac{\phi_1^2}{\sigma_2^2} - \frac{\phi_3^2}{\sigma_3^2 - \sigma_2^2} = 1. \tag{64}$$

We note that the points where the derivatives  $\frac{d\phi_a}{dx}$  change sign according the system (4) are encoded in the super-potential itself, not in the metric as in elliptic coordinates. The  $\lambda_3 = 1$  face, the ellipsoid

$$\phi_1^2 + \frac{\phi_2^2}{\sigma_2^2} + \frac{\phi_3^2}{\sigma_3^2} = 1 \quad ,$$

is a regular zone, however, in Cartesian coordinates.

Finally, it is easy to repeat the calculations in the  $N = 1$  and  $N = 2$  models to obtain the corresponding super-potentials in both elliptic and Cartesian coordinates. We shall include only the final results:

$$W^{(\beta_1, \beta_2)}(\phi_1, \phi_2) = (-1)^{\beta_1} \sqrt{\phi_1^2 + \phi_2^2 + (-1)^{\beta_2} 2\sigma_2\phi_1 + \sigma_2^2} \left[ \frac{1}{3} (\phi_1^2 + \phi_2^2 - (-1)^{\beta_2} \sigma_2\phi_1 + \sigma_2^2) - 1 \right]$$

$\beta_1, \beta_2 = 0, 1$ , are the super-potentials of the  $N = 2$  model obtained by reducing to the  $\phi_3 = 0$  plane the previously analyzed  $N = 3$  system. An analogous formula occurs in the  $\phi_2 = 0$  plane, whereas

$$W^{(\nu)}(\phi_1) = (-1)^\nu \left( \frac{1}{3} \phi_1^3 - \phi_1 \right) \quad ,$$

$\nu = 0, 1$ , are the super-potentials if the system is reduced to the  $\phi_2 = \phi_3 = 0$  axis.

## References

- [1] A. Alonso Izquierdo, M. A. González León and J. Mateos Guilarte, *Nonlinearity* **13** (2000), 1137.
- [2] E. Bogomolny, *Sov. J. Nucl. Phys.* 24 (1976), 449.
- [3] C. Montonen, *Nucl. Phys.* B112 (1976), 349.  
S. Sarker, S. Trullinger and R. Bishop, *Phys. Lett.* A59 (1976), 255.
- [4] D. Mumford, *L'Enseign. Math.* 23 (1977), 39.
- [5] D. Freed and K. Uhlenbeck, *Instantons and four manifolds*, Springer Verlag, New York, 1984.
- [6] M. Atiyah and N. Hitchin, *The geometry and dynamics of magnetic monopoles*, Princeton University Press, 1988.
- [7] M. A. Gonzalez Leon, *Integrable Systems and Geodesics: Solitons in the O(3) linear sigma model*. Ph D Thesis, Salamanca University, 2000
- [8] H. Ito and H. Tasaki, *Phys. Lett.* A113 (1985), 179.
- [9] J. Mateos Guilarte, *Lett. Math. Phys.* 14 (1987), 169, and, *Ann. Phys.* 188 (1988) 307.
- [10] D. Olive and E. Witten, *Phys. Lett.* B78 (1978), 97.
- [11] M. Giaquinta and S. Hildebrandt, *Calculus of variations, Volume I, Chapter 5, Section 2*, *Grundlehren der Mathematischen Wissenschaften*, Springer Verlag, 1996

- [12] M. Morse, Calculus of variations in the large, Amer. Math. Soc. Colloq. Publ., 1934.  
J. Milnor, Morse theory, Princeton University Press, 1963.
- [13] R. Bott, Bull. Amer. Math. Soc. 7 (1982) 331.
- [14] R. Garnier, Ren. Circ. Mat. Palermo 43 (1919) 155
- [15] M. Prasad and C. Sommerfield, Phys. Rev. Lett. 35 (1975) 760
- [16] J. Mateos Guilarte, Ann. Phys. 216 (1992) 122.